UPPSALA
UNIVERSITET

Digital Comprehensive Summaries of Uppsala Dissertations from the Faculty of Pharmacy 52

Pharmacodynamics of Enzyme Induction and its Consequences for Substrate Elimination

MATS O. MAGNUSSON

ACTA
UNIVERSITATIS
UPSALIENSIS
UPPSALA
2007

ISSN 1651-6192
ISBN 978-91-554-6860-6
urn:nbn:se:uu:diva-7812

Dissertation presented at Uppsala University to be publicly examined in B:41, BMC, Uppsala, Sweden, Friday, May 4, 2007 at 13:15 for the degree of Doctor of Philosophy (Faculty of Pharmacy). The examination will be conducted in Swedish.

Abstract
Magnusson, M O. 2007. Pharmacodynamics of Enzyme Induction and its Consequences for Substrate Elimination. Acta Universitatis Upsaliensis. *Digital Comprehensive Summaries of Uppsala Dissertations from the Faculty of Pharmacy* 52. 62 pp. Uppsala.
ISBN 978-91-554-6860-6.

Enzyme induction is a process whereby a molecule enhances the expression of enzymes. If the affected enzymes are involved in the elimination of a drug, this may result in a drug interaction. Induction is therefore of major concern during drug development and in clinical practice.

The induction process depends on the half-life of the induced enzyme, the pharmacokinetics of the inducing agent, and the relationship between the inducer's concentration and the induction stimulus. The aim of the conducted research was to investigate these key aspects of enzyme induction and the consequences that induction has for substrate elimination.

Successful investigations of the induction process presuppose the existence of appropriate methods for the estimation of the metabolic activity. Enzyme activity measurements can be conducted in tissues with low enzyme content using the analytical method presented here.

A model was developed describing the changes in the pharmacokinetics of clomethiazole and its metabolite NLA-715, that are attributable to carbamazepine induction. The consequences of the induction was explained using a mechanistic approach, acknowledging food-induced changes in the blood flow to the liver, and interpreting in vitro generated metabolic information.

The time course of the induction process was examined in two investigations. In the first of these, the pharmacokinetics of the autoinducing drug phenobarbital and its effect on several enzymes were described in rats. This was accomplished by integrating the bidirectional interaction between drug and enzymes in a mechanistic manner. In the final investigation, the time course of the increase and cessation in enzyme activity was studied in healthy volunteers treated with carbamazepine. This investigation allowed the half-lives of CYP3A and CYP1A2 to be estimated.

The key aspects of the enzyme induction process have been examined using mechanistic induction models. These novel models improve the understanding of the induction process and its consequences for substrate elimination.

Keywords: Pharmacokinetics, Pharmacodynamics, Enzyme induction, Time course, Turnover model, Mechanism-based, Modelling, NONMEM

Mats O. Magnusson, Department of Pharmaceutical Biosciences, Pharmaceutical Biochemistry, Box 578, Uppsala University, SE-75123 Uppsala, Sweden

ISSN 1651-6192
ISBN 978-91-554-6860-6
urn:nbn:se:uu:diva-7812 (http://urn.kb.se/resolve?urn=urn:nbn:se:uu:diva-7812)

Brilliant thoughts under the influence of Diet Coke

Till min familj, mest mamma!

Papers Discussed

This thesis is based on the following papers, which will be referred to in the text by the Roman numbers assigned below.

I M. O. Magnusson and R. Sandström. Quantitative analysis of eight testosterone metabolites using column switching and liquid chromatography/tandem mass spectrometry. Rapid Commun Mass Spectrom. 18: 1089-94 (2004).

II M. O. Magnusson, P-H. Zingmark, B. Fransson, M. O. Karlsson and, R. Sandström. A mechanistic model describing the impact of carbamazepine on the pharmacokinetics of clomethiazole and its metabolite NLA-715. *In manuscript.*

III M. O. Magnusson, M. O. Karlsson, and R. Sandström. A mechanism-based integrated pharmacokinetic enzyme model describing the time course and magnitude of phenobarbital-mediated enzyme induction in the rat. Pharm Res. 23: 521-32 (2006).

IV M. O. Magnusson, M-L. Dahl, J. Cederberg, M. O. Karlsson, and R. Sandström. Pharmacodynamics of enzyme induction attributable to carbamazepine treatment using midazolam, caffeine and digoxin as probes for CYP3A, CYP1A2 and P-glycoprotein. *In manuscript.*

Contents

Abbreviations

CYP	cytochrome P450
P-gp / ABCB1	p-glycoprotein
AhR	aryl hydrocarbon receptor
PXR	pregnane X receptor
CAR	consititutive androstane receptor
Arnt	AhR nuclear translocator
RXR	retinoid X receptor
CL	total clearance
CL_H	hepatic clearance
V	volume of distribution
k	elimination rate constant
Q_H	blood flow to the liver
f_u	ratio of unbound and total drug concentration
CL_{int}	intrinsic clearance
F_H	bioavailability across the liver
AUC	area under the plasma concentration-time curve
V_{max}	maximal metabolic rate
K_m	Michaelis-Menten constant
C_u	unbound concentration
A_{Enzyme}	amount of enzymes
R_{in}	production rate
k_{out}	elimination rate constant
$t_{½,Enzyme}$	half-life of an enzyme
C(t)	pharmacokinetic function
S	stimulus function
E_{max}	maximum effect/induction
EC_{50}	concentration one-half of the maximum effect
γ	shape factor in the Hill-equation
RT-PCR	reverse transcription polymerase chain reaction
mRNA	messenger ribonucleic acid
FOCE	first order conditional estimate method
ε_{ij}	difference between individual prediction and observation
η	difference between population and individual parameter estimate
θ	typical value of a parameter, fixed effect parameter
σ^2	variance of ε
ω^2	variance of η
LLOQ	lower limit of quantification
NADPH	nicotinamide adenine dinucleotide
EROD	etoxyresorufin
OHT	hydroxytestosterone
HPLC	high-performance liquid chromatography
MeOH	methanol
PB	phenobarbital
CBZ	carbamazepine

CBZ-E	carbamazepine-10,11-epoxide
DIG	digoxin
MDZ	midazolam
CAF	caffeine
PX	paraxanthine
TCDD	2,3,7,8-Tetrachlorodibenzo-*p*-dioxin
3-MC	3-methylcholanthrene
CV	coefficient of variation

Introduction

Background

The human body is constantly exposed to exogenous compounds in the food, in the form of environmental toxins and in the form of drugs. These xenobiotics can be harmful, so the body has developed several lines of defence against the toxins. The first defence mechanism is made of passive barrier organs, such as the skin, the gut-wall and the tight junctions in the capillaries leading to the brain, the ovaries and the testis. The second line of defence consists of active proteins in the form of enzymes and transporters. The role of the enzymes is mainly to make the xenobiotics more hydrophilic, thereby facilitating the excretion of the compounds. The transporters act as pumps and can prohibit the absorption of harmful compounds and/or enhance their elimination. Moreover, the active defence mechanisms can increase their effectiveness following exposure to certain xenobiotics. This process is known as enzyme induction. In most cases, the induction involves binding of the xenobiotic to a nuclear receptor, leading to increased protein synthesis, and a more effective protection against the compound. However, the induction is an unspecific process and, as a consequence, a drug with enzyme inducing properties might not only affect its own metabolism (a process known as autoinduction), but also the elimination of concomitant medications. Because of this, enzyme induction is a major concern in drug development and in clinical practice.

The magnitude of the enzyme induction has been studied in great detail using *in vitro* and *in vivo* methods, see for example references (1-4). *In vitro*, the activity or amounts of different enzymes can be measured by incubations with probe compounds or by western blots. In the clinic, the impact of induction can be assessed by measuring changes in the bioavailability and/or the elimination rates of the affected substrates before and after enzyme induction (5, 6). In these experiments, the enzyme activity is usually measured before and after a period of treatment with an inducing agent, so the magnitude of the induction on various enzymes is well-known for several inducing agents (4, 7). However, the time course of this process is inadequately described in the literature.

The pharmacodynamics of enzyme induction is complex. It depends on the half-life of the induced enzyme, the pharmacokinetics of the inducing agent, and the relationship between the plasma concentration of the inducer and the induction stimulus. If it is to be possible to predict the enzyme activity at any point in time during the induction process, all of these aspects have to be understood. By developing a model, the key elements of this system can be isolated, and their relative contribution to the induction process can be surveyed.

Biotransformation of Xenobiotics

The biotransformation of foreign compounds can be divided into three phases. In Phase I, the compound is made more polar, most commonly by means of oxidation, reduction or hydrolysis. This reaction can be catalyzed by, for example, cytochrome P450 (CYP) enzymes, monoamine oxidases or flavine oxidases. In Phase II, the compound is conjugated, with the end product being a large water soluble molecule, which in many cases is inactive. The final step in the elimination of xenobiotics is excretion, a process that may involve transporters that actively efflux the compounds into the urine or bile.

Cytochrome P450

The cytochrome P450 isoenzyme superfamily is quantitatively the most important, and the most studied Phase I metabolising enzyme. The proteins of the CYP-family consist of haemoproteins with a capacity to oxidize, reduce or hydrolyze numerous endo- and exogenous compounds. The first CYP-enzymes were found in the 1950s, when a hepatic microsomal pigment with an absorbance at 450 nm was identified (8-11). In 1963, the functional role of the CYP-enzymes for the oxidative metabolism of steroids and drugs was demonstrated (12, 13). After the CYP-enzymes had been identified, it was debated whether only one interchangeable form of the enzyme existed or if there where several different CYP-enzymes. Early induction experiments with phenobarbital (PB) and 3-methylcholanthrene (3-MC) proved the presence of several different CYP-enzymes (1, 2).

The CYP-enzymes are located on the endoplasmic reticulum and on the mitochondrial membrane inside the cell. The liver is the organ with the highest abundance of CYP-enzymes, but the presence of enzymes has also been demonstrated in the small intestine, pancreas, kidneys, lymphocytes, lungs, placenta, the testis barrier and the blood-brain barrier (14, 15). The CYP1, CYP2 and CYP3 families are the most abundant CYP-enzymes in the human liver, with about 80% of all oxidative metabolism of foreign compounds being attributed to one of these enzymes (16).

The CYP-enzyme activity of the small intestine has been studied with great interest in the last decade. The reason for this is that the gut-wall mucosa is the first line of defence against perorally dosed compounds. A drug interaction occurring in the gut-wall mucosa can, therefore, have dramatic consequences for the pharmacokinetics of drugs (17). About 82% of the human intestine's total CYP content consists of CYP3A, while 14% is CYP2C9 (18).

Phase II Metabolism

The metabolites produced by Phase I metabolism do not differ to a great extent from the parent molecule, as the initial metabolism has little impact on the weight and water solubility of the affected molecule. However, the oxidative reaction adds or exposes functional groups to which the Phase II enzymes can bind. The three most important Phase II reactions are sulfation, glucuronidation and glutathion conjugation, which are performed by sulfotransferase UDP-glucuronyltransferase, and glutathione-S-transferase, respectively (19). Both the Phase I and Phase II metabolism occur inside the cell, and the end result is a very large water soluble molecule that can hardly diffuse

across the cell membrane. Instead, the Phase II metabolites are actively effluxed by transporter proteins out of the hepatocyte into the bile or the sinusoidal blood.

Efflux Transporters

Repeated dosing of chemotherapeutic agents can, in many cancer cell lines, result in resistance. This is a phenomenon known as multi drug resistance, and, in 1976, it was shown to be caused by the efflux protein P-glycoprotein (P-gp, also known as ABCB1) (20). P-gp was found to actively transport chemotherapeutics, against a concentration gradient, out of the tumour cell. A decade later it was found that P-pg was not only expressed in tumour cells, but also in various organs in the body, e.g., the small and large intestine, the kidneys, the testis and the blood-brain barrier (21-24). In the kidney and liver, P-pg effluxes xenobiotics depositing them in the urine and bile, respectively. P-gp also acts as a gate-keeper in the intestine and in barrier organs, such as the testis barrier and the blood-brain barrier, to prevent harmful compounds from entering the body or, once in the body, from entering particularly sensitive organs. As mentioned above, the metabolites are often too hydrophilic to diffuse across the cell membrane after the Phase II metabolism, and are instead effluxed out of the cell. However, some compounds, such as digoxin, are substrates to P-gp without any prior metabolism.

P-gp is the most thoroughly investigated member of the ATP-binding cassette (ABC) superfamily of transporters. However, this superfamily contains, just like the family of CYP-enzymes, several members with different functional roles and locations. (25).

Overlapping Substrate Specificity

The CYP-enzymes have broad substrate specificity and a compound can often be a substrate to several enzymes. There is also an overlap in the substrate specificity between CYP-enzymes and P-gp (26). However, some compounds, such as midazolam and caffeine, have been documented to only be metabolised by a certain enzyme, making them useful as probes for investigations of specific enzyme's activity (5, 6, 27).

Mechanisms of Enzyme Induction

Enzyme induction is generally considered to be the result of *de novo* protein synthesis (28, 29). The mechanism of enzyme induction often involves a nuclear receptor, to which an inducing ligand binds and forms a complex. The complex then diffuses into the cell nucleus where it binds to the DNA and activates RNA polymerase, which then transcribes the genome. The end result can be a Phase I or II metabolising enzyme, or a transport protein. For a thorough description of the mechanism of enzyme induction, see, for example, the review by Handschin and Meyer (30).

Certain induction mechanisms do not involve any nuclear receptors, and are not the result of increased protein synthesis. For example, it has been suggested that the induction of CYP2E1 following the intake of alcohol is the result of enzyme stabilization (31, 32).

Nuclear Receptors and Inducible Proteins

The induction is, as mentioned above, generally the result of a nuclear receptor-ligand complex causing increased transcription of the genome. Different proteins are induced depending on which nuclear receptor is activated, and thereby, structurally different ligands can cause similar induction patterns.

The first nuclear receptor to be identified was the Aryl hydrocarbon Receptor (AhR), which dimerizes with the AhR nuclear translocator (Arnt). AhR is activated by several polycyclic aromatic hydrocarbons, such as the environmental toxin 2,3,7,8-tetrachlorodibenzo-p-dioxin (TCDD), which induces CYP1A1 and CYP1A2 (33, 34). Moreover, cigarette smoke is known to contain AhR-stimulating agents. In one study, the CYP1A2 activity was found to decrease by 34% following the cessation of smoking (35).

The Constitutive Androstane Receptor (CAR) was isolated by Baes et al. in 1994 (36), while the human Pregnane X Receptor (PXR) was found by Bertilsson et al. (37). Both CAR and PXR heterodimerize with the retinoid X receptor (RXR), and cause increased transcription of the genome associated with CYP2B, CYP2C and CYP3A. Pronounced CYP2B induction is related to CAR-activation, (38), while PXR-activation results in dramatic CYP3A induction (39). In addition, CAR and PXR has been shown to be involved in the regulation of efflux transporters (40).

Drug-drug Interactions

Inducing Drugs

In modern drug development, new candidate drugs are screened for their induction potential as a matter of routine. Induction is an unwanted property as it can cause interactions with concomitant medication and complicate the pharmacokinetics. Inducing drugs are, therefore, often not developed further. Still, there are a number of registered drugs with inducing characteristics, most of which were either developed before induction screening was introduced, or they are used in the treatment of diseases where there is an absence of alternative medication.

The most well-known enzyme inducing drugs of clinical importance are: the anticonvulsants carbamazepine, phenytoin and phenobarbital, the antifungal drug griseofulvin, the antimalarial artemether, the glucocorticoid dexamethasone, the antibiotics rifampicin and rifabutin, and the antidepressant herbal drug, St. John's wort. In addition, the antivirals ritonavir, nelfinavir and nevarapine, have inducing properties, but they are also simultaneously CYP-inhibitors. These opposite effects result in an initial decrease in the CYP-activity when treatment commences, but the enzyme levels increase as the inducing effect sets in.

The Consequences of Enzyme Induction

The first consequence of enzyme induction is increased elimination of the substrates of the affected enzymes. This leads to reduced plasma concentrations of the drug, resulting in a reduced drug affect. The second consequence of enzyme induction

regards the fate of the metabolites. The production rate of metabolites will, of course, be enhanced as the elimination of the parent compound speeds up, which can result in increased levels of the metabolite. As a result of this, if the metabolites can mediate an effect or cause toxicity, they must be monitored during enzyme induction investigations.

Important factors for determining the consequences of enzyme induction are the hepatic extraction ratio of the drug affected by induction, and the administration route. Enzyme induction will have limited impact on intravenously dosed high clearance drugs, because the systemic clearance is determined by the blood flow to the eliminating organ. However, induction might considerably reduce such a drug's bioavailability when it is dosed perorally. For a low clearance drug, the clearance is determined by the eliminating organ's efficiency, and induction will increase the systemic elimination, but will not affect the compound's bioavailability. This is all in agreement with the well-stirred model (41-43), which is described in Equations 1 and 2, where CL_H is the hepatic clearance, Q_H is the blood flow to the liver, f_u is the unbound fraction of the drug, F_H is the fraction of drug entering the liver that escapes elimination on a single passage through the organ, and CL_{int} is the intrinsic clearance value which is a metabolic efficiency measurement of the organ and is assumed to be increased by induction.

$$CL_H = \frac{Q_H \cdot CL_{int} \cdot f_u}{Q_H + CL_{int} \cdot f_u} \quad (1)$$

$$F_H = \frac{Q_H}{Q_H + CL_{int} \cdot f_u} \quad (2)$$

The liver is the most important drug metabolising organ, but gut-wall metabolism should not be overlooked as its importance was demonstrated in a study by Paine et al. (44), where it was found that the extraction ratio over the gut-wall mucosa was 43% in patients during liver transplantation. The bioavailability of CYP3A4 and P-gp substrates might be reduced extensively owing to induction in the gut-wall mucosa. (17).

Interactions Caused by Enzyme Induction

The clinical relevance of CYP3A4 induction has been investigated with great interest in the last decade as CYP3A4 is the most important drug metabolising enzyme. For example, in a well designed experiment, the prehepatic and hepatic induction of the CYP3A4 substrate verapamil was investigated before and after 11 days of rifampicin induction (17). The result was a 32-fold induction in the apparent S-verapamil clearance, and a 25-fold decrease in its bioavailability. The induction potential of rifampicin was further demonstrated in an investigation where the elimination of methadone, a hepatically cleared drug with a low clearance, was estimated before and after five days of rifampicin induction. The area under the plasma concentration-time curve (AUC) for methadone decreased by 70% following intravenous administration, while the peroral AUC decreased by 77% as a result of the rifampicin treatment. In a latter investigation, the effect of the PXR ligand, St. John's wort, on the elimination of the CYP3A4 substrate, midazolam, was evaluated by Wang and his colleagues (45). After two weeks of treatment with St. John's wort in healthy volunteers, the AUC of

midazolam had decreased by 50% when midazolam was given perorally, and by 20% when administered intravenously.

There are a few examples of clinically important CAR related drug interactions in the literature. For example, it was found that the AUC following an oral alprenolol dose decreased by an average of 80% after a 14 day induction period with pentobarbital (46). In a study by von Bahr et al, a greater than twofold increase in the nortriptyline clearance was found after a treatment period with pentobarbital (47).

Interactions Caused by P-glycoprotein Induction

Relatively few studies have been performed where the clinical importance of P-gp induction has been demonstrated. In one such investigation, though, the extent of P-gp induction was evaluated using digoxin as a probe following rifampicin mediated induction (48). It was found that the AUC following a peroral dose of digoxin decreased by a factor of 3.5 as a result of the rifampicin treatment. Moreover, the renal elimination of digoxin was unaffected by rifampicin. From this, it was concluded that the rifampicin induction altered the pharmacokinetics of digoxin by reducing the bioavailability. The inducibility of transporters was also demonstrated when the oral absorption of the P-gp substrate talinolol decreased as a consequence of carbamazepine treatment (49).

Enzyme Activity and Protein Abundance

Investigations of the induction process require the development of appropriate methods for the estimation of the metabolic activity or the protein content.

In Vitro Techniques

The activity of a specific enzyme in an organ can be estimated by incubating microsomes, prepared from the investigated organ, with probe substrates, metabolised by the CYP-enzyme of interest, (see, for example, references (50) and (51)). At low substrate concentrations, the elimination rate of the substrate or the formation rate of a metabolite is described by the V_{max}/K_m ratio, where V_{max} is the maximal metabolic rate and K_m is the Michaelis-Menten constant, determined by the enzyme's affinity to the substrate (52, 53). V_{max} is proportional to the amount of the enzyme and, hence, can be used as a measurement of the activity of the CYP-enzyme in the organ being investigated. Alternative methods for measuring the quantity of proteins are western blots (54), which can be used for the quantification of proteins, and RT-PCR (55, 56), which is suitable for measurements of mRNA levels. These *in vitro* techniques require that a sample of the investigated organ is obtained, making them of limited use in clinical experiments.

In Vivo Techniques

In humans, the enzyme activity can be measured by estimating the clearance of a probe. This is achieved by determining the ratio of the dose to the AUC, whereafter the CL_{int}

can be calculated from Equation 1. CL_{int} is related to V_{max} through Equation 3, where C_u is the unbound concentration of the substrate.

$$CL_{int} \;] \; \frac{V_{max}}{K_m \; / \; C_u} \tag{3}$$

The activity of a specific CYP-enzyme can be estimated if the probe used is metabolised only by a single CYP-isoform. The usefulness of cocktails of drugs, containing several probes that are metabolised, specifically, by certain CYP-enzymes, has been demonstrated for the measurement of several isoenzymes' activity in a single experiment (5, 6).

One drawback of the technique described above, though, is that several plasma concentration samples are required to obtain reliable estimates of the probe's AUC. This problem can, for certain probes, be circumvented by measuring the probe/metabolite concentration ratio at certain points in time. For some probes, this ratio has been shown to provide a valid surrogate measurement of the probe's clearance (57-60).

In Vitro-In Vivo Extrapolation

The metabolic characteristics of a new candidate drug are extensively investigated *in vitro* before it is administered to humans. The *in vitro* data obtained can predict some of the compound's pharmacokinetic properties. For example, the V_{max} and K_m of a drug can be estimated by measuring the rate at which the compound disappears when being incubated with human microsomes, whereafter CL_{int} can be calculated from Equation 3 (52, 53). By inserting the CL_{int} obtained for the drug, the blood flow to the liver, the blood/plasma concentration ratio and the fraction unbound into Equation 1, the clearance of the organ can be anticipated. A drawback of this technique, however, is that the calculated CL_{int} only represents the value for a few individuals, if individual microsome preparations are being used, or an average for a population, if the preparations have been pooled from numerous individuals. Because of this, the variability in CL_{int} can not be estimated with this method. However, this problem can be solved by incubating the drug with recombinant enzymes. From these incubations, each specific enzyme's CL_{int} can be estimated. Thereafter, the variability in CL_{int} in a population can be predicted by combining the CL_{int} of each enzyme with the distribution in the expression of these CYP-enzymes in the population. This latter approach has the additional advantage that the effect of drug-drug interactions can, to some extent, be foreseen (61, 62).

Pharmacodynamics of Enzyme Induction

In contrast to enzyme inhibition, enzyme induction is not an instant phenomenon. The reason for this is that it takes time to attain a new steady state condition between enzyme biosynthesis and enzyme degradation. In the 1970s, it was suggested that a turnover model can be applied to describe the time course of enzyme induction (28, 63, 64). The turnover model consists of a zero-order enzyme production rate (R_{in}) and a first-order elimination rate constant (k_{out}). The enzyme level at the steady state

is equal to the ratio of the production rate and the elimination rate constant (65). According to the turnover model, induction can be achieved either by increasing the R_{in}, or by inhibiting the k_{out}. Henceforth, only models that have an increased production rate will be discussed, since the induction is usually the result of *de novo* protein synthesis (66). Furthermore, it will be assumed that the inducing agent affects the amount of enzyme (A_{Enzyme}), which is proportional to V_{max}. V_{max} is related to CL_{int} through Equation 3, and CL_{int} is related to the clearance of the organ as expressed by Equation 1. The induction of A_{Enzyme} can, under these assumptions, be described by Equation 4, which is illustrated in Figure 1.

$$\frac{dA_{Enzyme}}{dt} = R_{in} \cdot S(C(t)) - k_{out} \cdot A_{Enzyme} \quad (4)$$

$$k_{out} = \frac{\ln 2}{t_{½,Enzyme}} \quad (5)$$

where C(t) is a pharmacokinetic sub-model for the inducing compound, S is the stimulus function, which relates the plasma concentration of the inducer to the induction stimulus, and $t_{½,Enzyme}$ is the half-life of the induced enzyme.

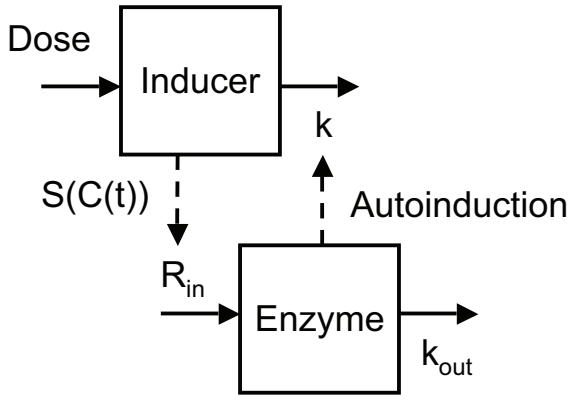

Figure 1 The turnover model, Dose is the dose rate of the inducing agent, k is the inducer's elimination rate constant, S(C(t)) is the relationship between induction stimulus and plasma concentration of the inducer, R_{in} is the zero-order production rate of enzyme, k_{out} is the first-order elimination rate constant of enzyme. In the case of autoinduction, the amount of enzymes will affect the elimination of the inducting compound, resulting in a bidirectional interaction.

Half-life of the Induced Enzyme

The turnover rate of the enzyme is often important for describing the time course of the induction process. This factor is determined by the half-life of the enzymes affected by the induction, and is independent of the characteristics of the inducer, making it a system specific parameter. The half-life of the CYP-enzymes has been estimated in a few investigations. Different *in vitro* and *in vivo* studies have reported the half-life of CYP3A4 to range from 72-140 hours (47, 64, 67-69). In one study,

the half-life of CYP1A2 was estimated to 28-54 hours in healthy volunteers following smoking cessation, using the paraxanthine/caffeine plasma concentration ratio as a measurement of the enzyme's activity (35).

In addition to the half-life of the induced enzyme, in order to adequately describe the induction process, both the pharmacokinetics of the inducer and the relationship between the plasma concentration of the inducer and the induction stimulus have to be considered. These two functions are drug specific, and are described in detail below.

Pharmacokinetics of the Inducing Agent

The plasma concentration of a compound, C(t), can be estimated at any given point in time using a pharmacokinetic model, for example, a one compartment model with a single intravenous dose, as in Equation 6.

$$C(t) = \frac{Dose}{V} e^{-kt} \tag{6}$$

where V is the volume of distribution, k is the CL/V ratio and t is the time elapsed since the dose was administered. From Equations 4 and 6, it can be anticipated that the time course of the induction process can be determined by k (when $k<<k_{out}$), by k_{out} (when $k>>k_{out}$) or by a combination of k and k_{out} (when $k \approx k_{out}$).

The Stimulus Function

The stimulus function, S(C(t)), relates the plasma concentration of a compound to the induction stimulus. A commonly used effect model is the E_{max} model, given in Equation 7 (70).

$$S(C(t)) = \frac{E_{max} \cdot C(t)}{EC_{50} + C(t)} \tag{7}$$

where S(C(t)) is the current induction stimulus, E_{max} is the maximal induction stimulus, C it the concentration of the inducer, and EC_{50} is the concentration that produces 50% of the maximal induction stimulus. The E_{max} model is physiologically plausible as it predicts no induction in the absence of the inducer, and there is a maximal induction, beyond which the induction stimulus is unaffected by a further increase in the concentration of the inducing compound. However, a wide range of concentrations is required to determine the components of the E_{max} model. If it is not possible to obtain such a wide range, and if the concentrations of the inducing agent can be assumed to be low in relation to EC_{50}, a linear model can be applied:

$$S(C(t)) = Slope \cdot C(t) \tag{8}$$

where "Slope" relates the concentration of the inducer to the current stimulus. The linear model predicts no induction in the absence of the inducer, just like the E_{max} model. However, no maximal induction stimulus is obtained with this model, which in many cases is not physiologically reasonable. The linear model should, therefore, not

be extrapolated to higher concentrations than those from which it was developed.

The hyperbolic shape of the Emax model can be altered by introducing a Hill factor (γ) to the sigmoidal E_{max} model, according to Equation 9.

$$S(C) = \frac{E_{max} \cdot C^{\gamma}}{EC_{50}^{\gamma} + C^{\gamma}} \quad (9)$$

The ordinary E_{max} model will be obtained for γ=1, while the the relationship between the induction stimulus and the concentration will be steeper for γ>1, and shallower for γ<1. The sigmoidal E_{max} model has great flexibility, but it might be difficult to determine the parameters of the model with accuracy. A special case of the sigmoidal E_{max} model occurs when high values are applied to γ. In this case, the model turns into an "all-or-nothing"-model, also known as a step model. With a step model, a maximal induction stimulus is predicted above a certain concentration, while no induction is predicted below a "cut-off" concentration, that is determined by EC_{50}. If the induction stimulus is at E_{max} at the start of the treatment with the inducer, a step model is usable during the onset of the induction. However, the model has limitations when the induction ceases, following withdrawal of the inducing agent, as the "cut-off" concentration then has to be estimated.

In the pentobarbital-nortriptyline induction model presented by von Bahr et al. (47), no plasma concentration measurements were obtained for the inducer, and therefore a step model was applied. Maximal induction was assumed when the subjects were treated with pentobarbital and it was assumed that there was no induction at all once the treatment had ended. In this study, the decrease in the concentration of nortriptyline was more rapid than the increase after the pentobarbital cessation. In the report, this is explained by the discrepancy in the half-life of nortriptyline during and after induction. However, it can be speculated that the pentobarbital inducing effect remained for some time after the inducer was withdrawn, as the half-life of pentobarbital is 24 hours (71).

In the cyclophosphamide autoinduction model that was presented by Hassan et al. (72), the induction magnitude is linearly related to the plasma concentration of cyclophsophamide as laid out in Equation 8, while an E_{max} model (Equation 7) was applied in the ifosfamide model presented by Kerbusch et al. (73).

Delayed Commencement

The commencement of enzyme induction involves a series of events leading to the production of new enzymes. Hence, a time delay between plasma concentration and the induction stimulus can be expected. Some *in vitro* experiments have addressed this issue. In one study, the mRNA levels were measured for CYP1A1, CYP1A2 and AhR following treatment with the environmental toxin, TCDD, or 3-MC in a human cell line culture (34). This study showed that the mRNA of the AhR nuclear receptor is unaffected by the inducer. Moreover, it was found that the initiation of the mRNA induction was rapid; the CYP1A mRNA levels increased significantly within one hour of 3-MC treatment and they were fully induced at six hours. The response from TCDD treatment was somewhat slower, with a moderate increase in mRNA being observed after 6 hours, and full induction being achieved within 24 hours.

A lag time can either be modelled as a step function, where the induction does not start until a "cut-off" at a certain point in time, or it can be modelled using a

transduction model (74, 75). The latter consists of a number of delay compartments introducing time lags between the enzyme production and the actual enzyme activity compartment. The flow between these compartments results in a delay between the time of the stimulus and the the measured increase in enzyme activity.

There are some enzyme induction models discussed in the literature which incorporate a delay between the stimulus and the start of induction. In the phenytoin autoinduction model by Frame and Beal (76), for example, a step model with no induction until an estimated "cut-off" point of 60 hours had been passed was used. This kind of step model was also used in the ifosfamide autoinduction model presented by Boddy et al. (77). In the work by Gordi et al. (78), a transduction model estimated the transit time between the stimulus and the start of induction to be two hours.

Induction Magnitude-Baseline Correlation

The R_{in} has to be representing the "true" production rate of the enzyme to obtain the A_{Enzyme} in Equation 4 in terms of a quantity of enzymes (e.g., in the unit amount of CYP-enzyme per amount of the organ). However, a genuine value for R_{in} is not easily obtained with current techniques. This can be circumvented by relating A_{Enzyme} at any point in time to the baseline measurement of A_{Enzyme}, which can be achieved by normalizing $A_{Enzyme, Baseline}$ to one, by letting R_{in} equal k_{out}. Thereafter, subsequent induction is proportional to $A_{Enzyme, Baseline}$. Alternatively, an inducible $A_{Enzyme, Inducible}$ can be separated from an uninducable $A_{Enzyme, Baseline}$, by letting R_{in} equal zero before induction. Here, the total A_{Enzyme} is the sum of the uninducible and inducible A_{Enzyme}, meaning that the baseline measurement is uncorrelated to the induction magnitude.

In the literature, there are examples of negative correlations between the baseline enzyme activity and the induction magnitude (79, 80). There can be several explanations for this: In the case of autoinduction, if the induction stimulus is dependent on the concentration of the inducer (as in Equations 7-9), the individual with the lowest baseline clearance will also be exposed to the highest concentrations of the inducing agent. This individual will thereby be induced to a larger extent than a subject with a high baseline clearance. This will cause a negative correlation between the baseline clearance and induction magnitude. Negative baseline to induction magnitude correlations can also be expected when the concentration of the inducer is close to E_{max} (Equations 7 and 9), or when the induced clearance approaches its maximal value (determined by the blood flow to the eliminating organ (Equation 1)).

A factor complicating the estimation of the relationship between the baseline enzyme activity and the induction magnitude is the presence of potential inducing agents in the environment, such as tobacco smoke, St. John's wort, environmental toxins and alcohol. Most individuals enrolled to a clinical trial are presumably contaminated with partly induced enzymes when the baseline enzyme activity is measured.

Pharmacokinetics of the Affected Drug

As explained above, the change in the amount of an enzyme can be predicted by combining the protein half-life, the pharmacokinetics of the inducer, and the relationship between concentration of the inducing agent and the induction stimulus. The outcome of the induction will also be dependent on the pharmacokinetics of the

drug affected by the induction, as a drug with a shorter half-life will respond more rapidly to a change in the enzyme activity than a drug with a longer half-life. This was described in a simulation study by Abramson (81), where it was illustrated how the half-life of the inducer, the half-life of the induced drug, or a combination of these, can determine the plasma concentration time profile for the compound affected by induction.

Non-linear Mixed Effect Modelling of Induction

The pharmacokinetic-pharmacodynamic relations of enzyme induction are complex and several factors have to be considered when anticipating the consequences of induction. By developing a model, the key elements of the enzyme induction system can be isolated, and their relative contribution to the induction process can be surveyed.

Mechanistic Models

Pharmacokinetic and pharmacodynamic modelling is, by its nature, based on physiological principles. Previously known structures and quantities can be included in a model to ensure that it is physiologically reasonable. The benefits of this kind of mechanistic model are that several sources of data can be merged into one model, where the underlying functional mechanism of the process under investigation might be understood. The components of the model can either be related to the drug or to the system being investigated. Examples of drug specific components are the pharmacokinetic and pharmacodynamic sub-models, while the system specific components could be a disease progression sub-model or the half-life of an enzyme affected by induction. By changing the drug specific components of a model to those of another drug, the consequences of the drug exchange on the system being investigated can be foreseen. Thus, the mechanistic model has the potential to be predictive beyond the range of the data on which it was developed (82-85).

Non-linear Mixed Effect Modelling

In traditional pharmacokinetic analysis a two-stage approach is applied, where a model is fitted to each individual separately, whereafter the inter-individual variability in the parameters is calculated (86-88). The drawbacks of this method are that extensive plasma sampling is required in all individuals and that different structural models might be applied to different individuals, which make the inter-individual variability calculations problematic. An alternative approach is to use non-linear mixed effect modelling, where at least two levels of variability (referred to as random effect parameters) are identified and separated. The first level of variability handles the residual variability, while the second one explains the differences between the subjects' parameter estimates. The model also includes structural parameters (referred to as fixed effect parameters), which are constant for all individuals. In non-linear mixed effect modelling, all fixed and random effect parameters are fitted simultaneously to all observations, allowing discrepancies in the data density, and the structure of the

model, between individuals. The drawbacks of this method are that it is computer intensive and time consuming.

The Structure of the Model

Observation j, for individual i is described by Equation 10.

$$y_{ij} = f(x_{ij}, P_i) + \eta_{ij} \quad (10)$$

where $f(x_{ij}, P_i)$ is a linear or non-linear function describing the individual prediction, with the parameter vector P_i and independent variables x_{ij}. For a pharmacokinetic model, P_i typically consists of an absorption rate constant, volume of distributions and clearances, while x_{ij} can be the dose and time. ε_{ij} is a random effect variable, which is defined as the difference between the individual prediction and the actual measurement of observation j for individual i. ε_{ij} is assumed to be normally distributed, with a mean of zero, and variance of σ^2. Alternative forms of the random effect variable are possible (89). P_i consists of several model parameters where, the inter-individual variability in a parameter k for individual i (p_{ki}) can be can be described by Equation 11 for a normally distributed parameter. However, many physiological parameters are log-normally distributed, in which case Equation 12 can be used to describe the inter-individual variability in a parameter.

$$p_{ki} = \tau_k + \kappa_{ki} \quad (11)$$

$$p_{ki} = \tau_k \cdot e^{\kappa_{ki}} \quad (12)$$

where θ_k is the parameter of the typical individual and η_{ki} is the difference between the i^{th} individual's parameter estimate and the value for the typical individual. η_{ki} is assumed to be normally or log-normally distributed with a mean of zero and variance of ϖ_k^2. Sometimes, patients' characteristics, such as their body size or kidney function, can explain some of the discrepancy in the parameter estimate between individual i and the typical individual. These characteristics are referred to as covariates and can be included in Equations 11 or 12.

Characteristics of Compounds

Inducing Agents

Phenobarbital

Phenobarbital is used in the treatment of epilepsy, and has well-documented enzyme inducing properties. Phenobarbital is a ligand to the CAR receptor, through which it causes strong CYP2B6 induction and, to a lesser extent, induction of CYP2C9 and CYP3A4 (90). Phenobarbital is known to inhibit the CYP2C11 enzyme activity in the

rat. The mechanism behind this inhibition is not completely understood, but it might involve a phenobarbital-mediated depression of the growth hormone pulses (91). In humans, phenobarbital is metabolised by CYP2C9, CYP2C19 and CYP2E1, and, as it causes induction in CYP2C9, it has autoinducing properties (92-94).

Carbamazepine

Carbamazepine is a commonly used antiepileptic drug. Its quantitatively most important metabolic pathway is a CYP3A4 and CYP2C8 catalysed epoxidation to carbamazepine-10,11-epoxide (CBZ-E) (95), which is then further metabolised by epoxide hydrolase and extracted in the urine. Carbamazepine is a potent inducer of CYP3A4, which contributes to the carbamazepine epoxidation. Hence, CBZ has autoinducing properties leading to complex pharmacokinetics. Moreover, according to some reports, CBZ induces CYP1A2 (96) and the efflux protein P-gp (49).

Probe Substances

Testosterone

Different CYP-enzymes form single-hydroxylated testosterone metabolites (OHT), making testosterone useful as an *in vitro* probe for simultaneous estimation of the activity of several enzymes in one incubation experiment. The testosterone metabolites are believed to be associated with CYP-enzymes as follows: 2β-OHT with CYP3A1/2; 6α-OHT and 7α-OHT with CYP2A; 16β-OHT with CYP2B1/2; 2α-OHT with CYP2C11. 16α-OHT is a substrate for both CYP2B1/2 and CYP2C11. The formation of androstenedione is associated with CYP2B1/2 and CYP2C11 (97-101).

Resorufin

The formation rate of resorufin from etoxy-resorufin is a commonly used reaction for the estimation of CYP1A2 enzyme activity (102).

Midazolam

Midazolam is a hypnotic benzodiazepine. The hydroxylation of MDZ to 1-OH-midazolam is a well-known specific marker of CYP3A4 activity (103).

Caffeine

A commonly used substrate for CYP1A2 activity is the metabolism of caffeine to paraxanthine (5, 6, 27).

Digoxin

Digoxin is a cardiac glycoside. The utility of using digoxin as a P-pg probe has been demonstrated in several studies (48, 104). Moreover, co-administration of digoxin and midazolam has recently been shown to be useful for simultaneous phenotyping of P-gp and CYP3A4 (58).

Aims

The general aim of the research conducted for this thesis was to investigate the key aspects of enzyme induction and the consequences that induction has for substrate elimination by using non-linear mixed effect models.

The specific aims were to

- Develop a sensitive analytical method, suitable for the analysis of testosterone hydroxylase activity, in order to quantify enzyme activity in various tissues.
- Utilize *in vitro* generated metabolic characteristics of clomethiazole and its metabolite NLA-715 in the development of a mechanistic pharmacokinetic model, and, thereby, to explain the pharmacokinetics of the compounds before and after carbamazepine-mediated enzyme induction.
- Characterize the pharmacodynamics of phenobarbital-mediated enzyme induction and to develop an integrated pharmacokinetic-enzyme model describing the changes in the activities of specific CYP-enzymes.
- Describe the characteristics of carbamazepine autoinduction and the pharmacodynamics of the carbamazepine-mediated induction of CYP3A4, CYP1A2 and P-gp.

Materials and methods

Experimental Procedures
Preclinical Investigation (Paper III)

Animals

Male Sprague-Dawley rats (Charles River, Uppsala, Sweden) weighing 250-300 g were used. The animals were acclimatized for at least 7 days prior to the experiment. They were maintained at 22 °C in a humidity controlled room with a 12-h light/dark cycle and free access to food and water. The animals were treated according to the Principles of Laboratory Animal Care, and the Animal Ethics Committee at the court in Tierp, Sweden, approved the protocol before the study was initiated.

Dosage and Sampling

The rats were randomized into five groups of eight animals per group. The animals received intraperitoneal (i.p.) injections of phenobarbital (Fenemal Recip® 200 mg/mL, 80 mg/kg body weight) once daily for 1, 2, 4, 9, or 14 consecutive days. Four rats were used as controls and received i.p. injections of saline. A 100 µL plasma sample was withdrawn, by vein puncture in the hind pawn, from each animal, daily. After the last dose of PB, ten plasma samples were withdrawn within the next 24 h. The rats were decapitated 24 h after their last injection of PB. The livers were harvested immediately after decapitation from four rats in each treatment group and from the four control animals. The livers were stored in TRIS buffer at -80 °C until microsomes were extracted from the livers.

Microsome Preparation and Incubations

Microsomes were extracted from 24 livers individually using different centrifugation steps according to the procedure described by Meijer et al. (105). The protein content in the microsome solution was determined in triplicates with the method developed by Lowry et al. (106) using bovine serum albumin as the standard.

Incubations were carried out at 37 °C in a 60-rpm shaking water bath (Haake SWB 20, Fisons, Karlsruhe, Germany). The microsomes were added to a final protein concentration of 0.1 mg/mL in TRIS buffer containing 1 mg/mL NADPH. The incubation solution was preincubated for 3 min before the substrate was added. EROD and testosterone were added to final concentrations of 4 and 100 µM, respectively,

in separate incubation vials. Moreover, incubations were performed with the formed metabolites of EROD and testosterone.

Estimation of the Activity of the CYP-enzymes

The formation rates of the probe compounds were estimated as follows: First, the metabolic rates with which resorufin, 2α-, 2β-, 6α-, 7α-, 16α-, and 16β-OHT, and androstenedione were metabolised were estimated as a first-order process. Then, on the basis of the incubations with EROD and testosterone, the formation rates of resorufin, 2α-, 2β-, 6α-, 7α-, 16α-, and 16β-OHT, and androstenedione were estimated using both the appearance of the metabolites and the previously estimated metabolic rates (now fixed) of the metabolites. A decrease in formation rate, not attributable to a decrease in substrate levels, was observed during the 40 min incubation period, so a linear loss of enzyme activity over time was added to the model. The individually estimated initial formation rates of the functional markers were used as measurements of the enzymes' activity in the further modelling process. Thereby, four data points (one per animal) were generated for each functional marker at induction days 0, 1, 2, 4, 9, and 14.

Experimental Procedures
Clinical Investigations (Papers II and IV)

The clinical studies were conducted on male Caucasian volunteers, who had been declared healthy after a physical examination. All subjects had given informed consent, and the trials were approved by local ethics committees and the Swedish medical products agency.

Carbamazepine-Clomethiazole Interaction Study (Paper II)

Sixteen subjects received a ten-hour infusion of clomethiazole (24 mg/kg·h for 15 minutes followed by 3.59 mg/kg·h for 9.75 hours) on two occasions. Clomethiazole and NLA-715 plasma samples were frequently drawn during the twenty-four hours immediately following the initiation of the infusions. Twelve subjects were treated with carbamazepine for 14-19 days between the two infusions, while four subjects received placebo. The carbamazepine dose was individually titrated, aiming for a carbamazepine plasma concentration of 15-40 µmol/L, which is regarded as a therapeutically active concentration (107).

Carbamazepine–Drug Cocktail Interaction Study (Paper IV)

Seven subjects received 200 mg carbamazepine (Tegretol®, Novartis) for two days, followed by 400 mg carbamazepine for 14 days. All CBZ doses were taken once per day and were administered around 8 pm, with the exact time being recorded. Henceforth, the various days on which the study took place will be referred to as day -3 to 30, where day 0 is defined as the day of the first carbamazepine dose. Days preceding the first carbamazepine dose, on which baseline measurements were made,

have negative values. The last carbamazepine dose was taken on day 15. The activity of CYP3A4, CYP1A2 and P-gp was assessed by dosing of a cocktail of drugs containing midazolam (1 mg/mL oral solution (Apoteket Produktion & Laboratorier, Sweden), caffeine (Koffein Recip®, Recip) and digoxin (Lanacrist®, AstraZeneca) on days -3, 1, 2, 3, 5, 11, 16, 17, 18, 24 and 30. Venous blood samples were collected from each subject by vein puncture in the arm for quantification of the investigated compounds 5 min before the cocktail of drugs was given and 4 and 8 hours after the dose. In addition, blood samples were collected 0.5, 1 and 2 hours after the dose of cocktail was administrated on days -3, 1 and 16.

Chemical Analysis

All of the analyses were conducted using high-performance liquid chromatography (HPLC) systems consisting of a Triathlon refrigerated autosampler (Spark, Emmen, Holland) and LC-10AD pumps (Shimadzu, Kyoto, Japan). The different chemical assays are described in detail in their respective paper.

Eight Metabolites of Testosterone (Papers I and III)

An external six-port valve was attached to the autosampler, allowing for online desalting and cleaning of the samples. The column-switching procedure, similar to a setup described by Tachibana and Tanaka (108), is illustrated in Figure 2. The samples were loaded onto the purification column (Zorbax SB-CN column, 12.5 x 4.6 mm i.d., 5 µm particle size) using a 5% methanol mobile phase. After five minutes of desalting and cleaning on the purification column, the sample was transferred to the analytical column (Zorbax SB-CN column, 250 x 4.6 mm i.d., 5 µm particle size), using the column switching procedure. The analytes were separated using a high-pressure linear gradient, with the mobile phase changing from 33% methanol to 40% methanol during the first 20 min and then rising to 55% methanol from 20–33 min. The concentration of ammonium acetate was 0.5 mM in all mobile phases. The flow rate through both columns was 1 mL/min throughout the analysis.

The flow from the analytical column was split 1:5, with 200 µL/min directed to a triple-quadrupole mass spectrometer (Quattro Ultima, Micromass, Manchester, UK). The ion-spray interface was held at 350 ºC, using nitrogen as the nebuliser and auxiliary gases. All analytes were ionized by positive ion electrospray (4500 V) and detected by mass spectrometry using multiple reactions monitoring.

Phenobarbital and Resorufin (Paper III)

Quantification of phenobarbital plasma concentrations was performed using a modified version of a previously reported method (109). An ultraviolet detector at wavelength 240 nm and a 10 x 4.6 mm, 5 µm particle size, Chromosphere C18 column, was used. The mobile phase consisted of 30% methanol in water.

The resorufin was quantified using a method modified from Leclercq et al. (110), using a fluorescence detector (excitation and emission wavelengths were set at 530 and 580 nm, respectively) and a 10 x 4.6 mm, 5 µm particle size C4 column. The mobile phase consisted of 58% 25 mM phosphate buffer (pH 7.0) and 42% methanol.

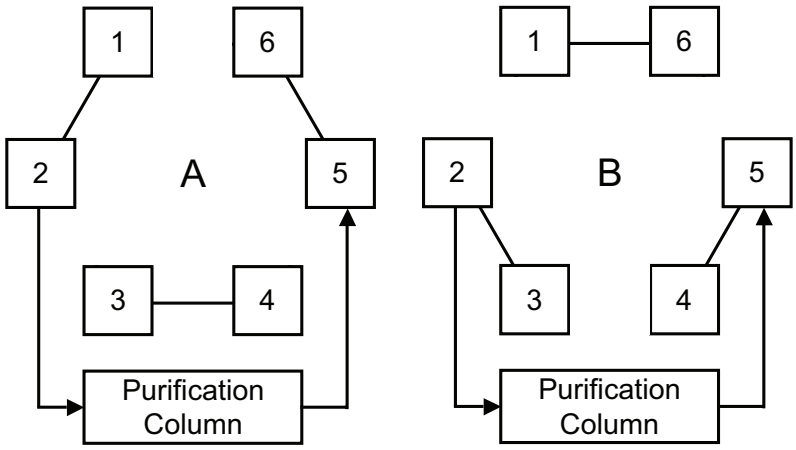

Figure 2. The column-switching setup. 1: Pump A (5% MeOH) and autoinjector; 2: purification column in; 3: pump B (gradient 33–55% MeOH); 4: analytical column and MS/MS; 5: purification column out; and 6: waste.

Clomethiazole, NLA-715 and Carbamazepine (Paper II)

The determination of the clomethiazole and NLA-715 concentrations in plasma was performed by the Department of Bioanalysis, AstraZeneca R&D, Södertälje, Sweden, while the carbamazepine levels were determined at Huddinge University Hospital, using routine methods for carbamazepine therapeutic drug monitoring.

Carbamazepine and the Cocktail of Drugs (Paper IV)

The plasma concentrations of carbamazepine, carbamazepine-10,11-epoxide, midazolam, 1-hydroxymidazolam, caffeine and paraxanthine was analysed by a modified version of a method described by Scott et al. (27), while the digoxin concentrations were measured according to a method described by Yao et al. (111). Separation was achieved using a 3 µm particle size, 50 x 4.6 mm, reversed phase analytical column (HyPurity C18, Thermo Hypersil-Keystone, PA, USA), protected by a 10 x 4 mm guard column of the same material as in the analytical column. A triple quadrupole mass spectrometer (Quattro Ultima; Micromass, Manchester, UK) was used as a detector.

Validation of Chemical Assays

The intra-day precision and accuracy of the methods developed at Division of Pharmacokinetics and Drug Therapy, Uppsala University, were determined in validation runs. These runs included one calibration curve, and determination of the concentrations of quality control samples were done in six replicates. To determine the variability at the lower limit of quantification (LLOQ) the analysis of the lowest concentration standard was replicated six times in addition to its determination for

purposes of the standard curve. The precision of the method at each concentration was expressed as the coefficient of variation (CV) by calculating the standard deviation as a percentage of the mean calculated concentration. The accuracy was determined by expressing the mean calculated concentration as a percentage of the added concentration.

Data Evaluation

All pharmacokinetic and pharmacodynamic information collected in this thesis has been evaluated by means of nonlinear mixed-effect modelling using maximum likelihood estimation in the computer program NONMEM, version VIβ (112). The first-order conditional estimation (FOCE) method was used throughout all the analysis. The estimated population model parameters were: i) the fixed-effect parameters related to the typical individual and ii) the random-effect parameters, describing the magnitudes of inter-individual variability in parameters (exponential models) and the residual variability between individual predictions and observations (proportional and/or additive models). The development of non-linear mixed effect pharmacokinetic models is by nature an iterative process. However, the following general strategy for the analysis has generally been used: First, reasonable models for the basic population characteristics were developed. Secondly, the variability between the subjects of the study was added and finally the influence of covariates on the pharmacokinetic parameters was evaluated.

The difference in the objective function value produced by NONMEM was the main tool used to discriminate between two nested models. A drop in the objective function value (-2·log-likelihood) of more than 3.84 between two nested models corresponds to $p < 0.05$, which was regarded as a statistically significant improvement. However, a drop of 3.84 has been shown to not correspond to $p < 0.05$ for datasets with few individuals (113). Therefore, a more conservative view of the drop in the objective function value was applied in datasets with few individuals. In addition to the NONMEM produced objective function value, the model-building process was guided by graphical evaluation using S-Plus version 6.1 (Insightful, Seattle, WA) with the Xpose library, version 3.1 (114), as well as a judgment of reasonable parameter estimates and their corresponding standard errors.

The uncertainty in the parameter estimates were presented as the NONMEM produced standard errors in Paper II. In Paper III and IV, the NONMEM-generated standard errors of the final parameters in the models were confirmed by bootstrapping 200 samples. The bootstrap was performed by resampling on the individual level using the PsN toolkit (115). Fixed and random effects parameters as well as standard error estimates of the final model were compared to the bootstrap results.

Modelling Procedures

Model for Carbamazepine-Clomethiazole Interaction (Paper II)

The clomethiazole-NLA-715 model contained one liver compartment each for clomethiazole and NLA-715, allowing a mechanistic approach to be adopted in the modelling process (see Figure 3 for the final structural model), as described by Gordi et al. (78). All elimination was assumed to take place in the liver compartments and was described by the well-stirred model (Equation 1). The liver blood flow was set to 100 L/h in all individuals (116). However, the subjects were served food four hours after the start of the infusion. It has been reported that eating food increases the blood flow to the liver by 40% (116). Therefore, the liver blood flow was changed to 140 L/h from four hours after the start of the infusion, and kept at that rate during the rest of the sampling period. The clomethiazole plasma protein binding is 63 ± 1.6% (117), so the f_u was set to 37% for this compound. The NLA-715 plasma protein binding is unknown, but was assumed to be the same as for clomethiazole. It has been reported that the blood to plasma concentration ratio (Cb/Cp) is 0.76 for clomethiazole (117). The concentration measurements were done in plasma, and they were therefore transformed to blood concentrations, and the f_u was transformed to its equivalent f_u in blood, in the NONMEM control stream.

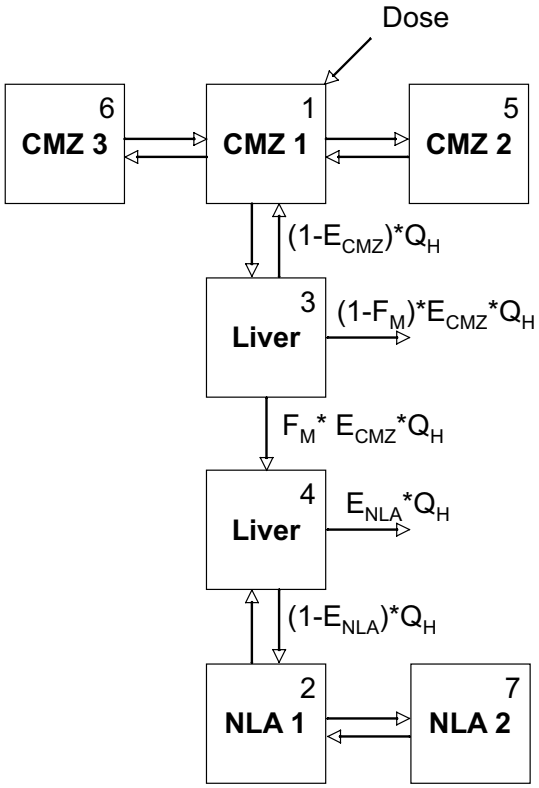

Figure 3 The structure of the final clomethiazole model. CMZ and NLA refer to the compartments associated with clomethiazole and NLA-715 respectively. E_{CMZ} and E_{NLA} are the compounds extraction ratios, Q_H is the blood flow to the liver and F_M is the fraction of clomethiazole being metabolised to NLA-715.

Linear and non-linear (Michaelis-Menten) kinetic models, according to Equation 13a (linear), 13b (non-linear) or 13c (non-linear-two compounds competing for the same enzyme), were evaluated as the best predictor of the elimination of clomethiazole and NLA-715.

$$CL_{\text{int}} = \frac{V_{\max}}{K_m} \tag{13a}$$

$$CL_{\text{int}} = \frac{V_{\max}}{K_m / C_u} \tag{13b}$$

$$CL_{\text{int},a} = \frac{V_{\max,a}}{K_{m,a}\left(1 + \frac{C_{u,b}}{K_{m,b}}\right) / C_{u,a}} \tag{13c}$$

where V_{max} represents the maximum metabolic rate, K_m is the unbound concentration giving half of the maximal metabolic rate, C_u is the unbound concentration of the substrate. The change in the compound's elimination rates attributable to the carbamazepine treatment was assumed to be proportional to the preinduced V_{max} for each metabolic route.

Model for Phenobarbital Induction (Paper III)

The phenobarbital model was developed in steps. Initially, the pharmacokinetics of PB was modelled after a single PB dose, without an autoinduction model. Thereafter, data following repeated PB dosing was modelled, and an autoinduction model was introduced. Step models, linear and non-linear models were evaluated for the phenobarbital exposure-induction stimulus relation (Equations 7-9). The presence of a lag time for the initialization of the enzyme induction was evaluated with a step model as well as a transduction model (75), using two transition compartments.

When the model of the pharmacokinetics of PB and its autoinduction had been established, the influence of PB exposure on the activities of the different CYP-enzymes was examined. The time course of the changes in the activities of the enzymes was modelled with a turnover model (Equation 4). The effect of PB exposure on the production rate (R_{in}) and the turnover rates (k_{out}) of the enzymes was evaluated with step models, linear and non-linear models (Equations 7-9), and the presence of a lag time for the initialization of the induction was assessed.

As a final step, an integrated model, including the pharmacokinetics of PB, its effect on the activities of the CYP-enzymes, and the influence of the CYP-enzymes on the elimination of PB, was estimated simultaneously. Thereby, the autoinduction of PB was estimated via the PB-dependent changes in the activities of the enzymes. The CYP-enzymes were included one by one in the model, in order to find which enzymes that best described the autoinduction of the PB elimination.

Model for Carbamazepine-Drug Cocktail Interaction (Paper IV)

The sum of the amounts of CBZ and CBZ-E was assumed to affect the induction magnitude. The drug exposure-induction stimulus function was evaluated with

step models, linear models and E_{max} models (Equations 7-9). The time course of the induction was described by a turnover model (Equation 4). The intrinsic clearances of the compounds under investigation were assumed to be proportional to the amount of enzyme in an enzyme compartment.

Digoxin

The pharmacokinetics of digoxin were evaluated with first-order absorption and an ordinary linear elimination model, parameterised in terms of the clearance and the volume of distribution.

Carbamazepine

The pharmacokinetics of CBZ and CBZ-E were described by a model with first-order absorption and an elimination model, similar to the model used for digoxin. The fraction of CBZ being metabolised to CBZ-E (F_M) has been reported to be 20% after a single CBZ dose, but it increases with the number of doses as a consequence of enzyme induction (118). This was handled in the model by letting the sum of two CBZ clearance values describe the elimination of CBZ, the first being an inducible clearance (CL_{CBZ1}), which was assumed to form CBZ-E and the other being an uninducible clearance (CL_{CBZ2}), which was fixed prior to induction to be four times higher than CL_{CBZ1}. CL_{CBZ2} was assumed to form metabolites that were not quantified in the chemical analysis.

Midazolam

Midazolam is known to be metabolised in the gut-wall mucosa before entering the liver (119), so a gut-wall compartment was inserted between the dosing compartment and the sampling compartment. The extraction ratio over the gut-wall (E_G) was estimated for MDZ according to Equations 14-15

$$E_G = \frac{CL_{int,G} \cdot f_{u,G}}{Q_G + CL_{int,G} \cdot f_{u,G}} \tag{14}$$

$$F_G = 1 - E_G \tag{15}$$

where $CL_{int,G}$ is the intrinsic clearance of the gut-wall, $f_{u,G}$ is unbound fraction in the gut-wall, fixed to 1 in the model, and Q_G is the rate of drug transport over the gut-wall mucosa, which was also fixed to 1. The MDZ gut-wall extraction ratio has been reported to be 43% (119), and therefore, the preinduced $CL_{int,G}$ was fixed to 0.754. The half-life of the gut-wall mucosa has been reported to be 24 hours (120) and half-life of the gut-wall induction process was therefore fixed to this value.

Midazolam has an intermediate extraction ratio, so hepatic enzyme induction will affect both the bioavailability and the systemic clearance of this compound. A liver compartment was, therefore, inserted between the gut-wall compartment and the sampling compartment. The liver compartment allowed the development of a semi-physiological model of the type described in detail by Gordi et al. (78). The systemic MDZ elimination was assumed to occur in the liver compartment, with an extraction ratio and clearance described by the well-stirred model (Equation 1). The f_u was assumed to be 5% in plasma (121), the blood to plasma concentration ratio

was assumed to be 0.7 (122), and the blood flow to the liver was set to 100 L/h in all individuals (116). Since the MDZ concentrations were measured in plasma, these observations were transformed to blood concentrations, and the f_u was transformed to its equivalent f_u in blood, in the NONMEM control stream.

Caffeine

The pharmacokinetics of caffeine and paraxanthine were modelled with a semi-physiological model in which one liver compartment was used for each substance, in a similar way to that adopted by the MDZ model. The unbound fraction was assumed to be 68% for CAF and 54% for PX, with a blood to plasma concentration ratio of 1 (123). The fraction of CAF metabolised to PX was set to 84% (124) and was assumed not to change as a result of enzyme induction.

Results and discussion

Quantification of Eight Metabolites of Testosterone (Paper I)

Full separation of the eight testosterone metabolites was achieved with a run time of 32 minutes on the column (Figure 4). The calibration curves for all metabolites were found to be linear over the investigated concentration ranges, with a regression coefficient greater than 0.997 for all investigated compounds. The intra-day CVs were between 3.5 and 17.9% at the LLOQs, and the accuracy at the LLOQs ranged from 88.0–104%.

A MS/MS spectrometer is a very sensitive detector. However, the main advantage of the MS/MS detector is its ability to differentiate molecules with different molar masses. Full chromatographic separation is, therefore, usually not required. In this study, however, the only compound with a unique precursor-to-product MS/MS fragmentation was androstenedione. All other compounds share their precursor mass with their isomers, and also form similar fragments at the collision energies used in this study. Therefore, full chromatographic separation of all hydroxylated testosterone metabolites was required.

The sensitivity of the analytical method was prioritised to short run times in this work. From the initial tuning, it was evident that other organic solvents than methanol suppressed the signal from the hydroxylated testosterone metabolites. It was therefore decided that no other solvent than methanol was to be used to separate the testosterone metabolites on the analytical column, even though other methods have been presented with good separation with short run times, using organic solvents such as acetonitrile and tetrahydrofuran (108, 125).

Direct injection of the incubation media containing TRIS-buffer and NADPH resulted both in immediate decreased sensitivity and declining sensitivity over time, likely caused by salts depressing the signal. Therefore, an automated column-switching procedure was used to desalt and clean the samples. The recovery from this procedure was >99.8% for all compounds. The column switching enabled injection of samples directly from the incubations, requiring no sample preparation other than a 5 minute centrifugation to remove proteins. This is an easy and rapid sample preparation, and makes the total amount of time spent on each sample reasonable despite the long analytical run time.

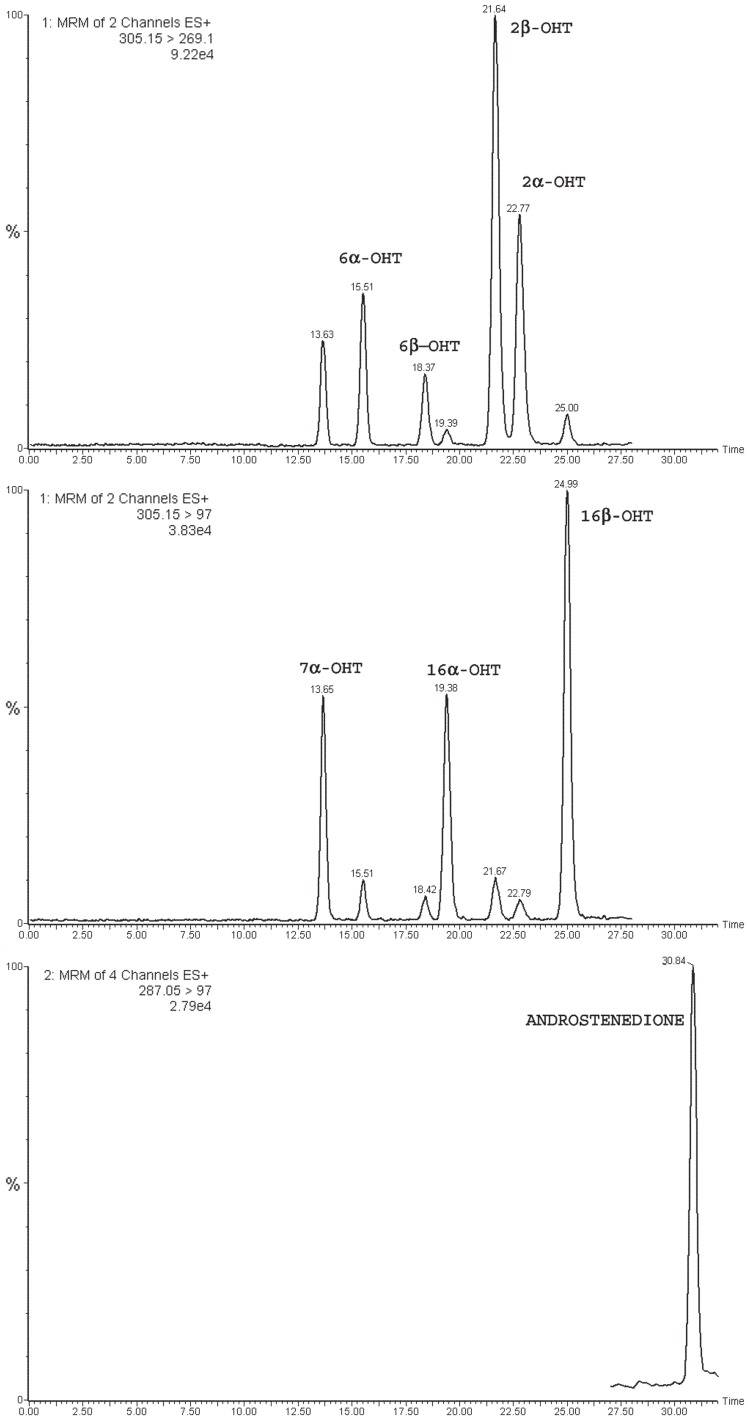

Figure 4 Example of chromatographic separation of testosterone metabolites of QCC from the validation assay. (A) Transition m/z 305.15>269.1; (B) transition m/z 305.15>97.0; and (C) transition m/z 287.05>97.0.

Assessment of Enzyme Activity

In Vitro

In Paper III, the activities of the enzymes were estimated using incubations of microsomal proteins with testosterone and etoxyresorufin. Initially, the evaluation of the production rates of the probes resulted in negative trends in the individual residuals vs. incubation time plots. However, by introducing sequential metabolism for the metabolites, and a loss in the enzyme activity during the 40 minute incubation period, the enzymes' activities could be estimated. PB does not only induce Phase I metabolism through CYP-enzymes, but it can also induce Phase II metabolism (126, 127). It was, therefore, necessary to measure the PB-mediated changes in the metabolism of the formed metabolites. However, the sequential metabolism of the metabolites could not fully explain the bent concentration-time curve. By estimating a linear decrease in enzyme activity over time, well-fitted concentration-time plots could be obtained.

In Vitro-In Vivo Extrapolation

In Paper II, an extrapolation to human liver was performed from *in vitro* incubations performed with clomethiazole and NLA-715 (128), using the Simcyp Clearance and Interaction Simulator®, version 6 (61). Simcyp® predicted that, because of enzyme saturation, there would be a 50% decrease in CL_{int} for CYP2A6 at the clomethiazole concentrations reached at the steady state, while the CL_{int} values for the other CYP enzymes were unchanged. Based on this knowledge, three elimination routes were estimated for the clomethiazole metabolism, and one for the NLA-715 metabolism, resulting in the following parameters: $CL_{int\ CYPY}$, (linear elimination of clomethiazole to NLA-715), $CL_{int\ CYPX}$ (linear elimination of clomethiazole to unmeasured metabolites), $V_{max\ CYP2A6\text{-}CMZ}$ (non-linear elimination of clomethiazole to NLA-715), $K_{m\ CYP2A6\text{-}CMZ}$ (affinity of CYP2A6 for clomethiazole), $V_{max\ CYP2A6\text{-}NLA}$ (non-linear elimination of NLA-715) and $K_{m\ CYP2A6\text{-}NLA}$ (affinity of CYP2A6 for NLA-715). Clomethiazole and NLA-715 were both assumed to be competitively metabolised by the saturable enzyme CYP2A6. Thus, $CL_{int\ CYP2A6\text{-}CMZ}$ and $CL_{int\ CYP2A6\text{-}NLA}$ were calculated using Equation 13c. Moreover, after the clomethiazole infusion had ended, the NLA-715 plasma concentrations declined exponentially, indicating that the kinetics for this compound were linear. Therefore, the $K_{m\ CYP2A6\text{–}NLA}$ was fixed to a high value (200 µmol/L). Still, as clomethiazole and NLA-715 are competitively metabolised by CYP2A6, the NLA-715 metabolism is saturated at high clomethiazole concentrations. However, the clomethiazole concentrations decline rapidly when the infusion is stopped, which makes first-order elimination of NLA-715 possible when the infusion has ended.

In Vivo

The activity of CYP3A, CYP1A2 and P-glycoprotein were measured by using midazolam, caffeine and digoxin as probes, in Paper IV. Moreover, the metabolites 1-OH-MDZ, 1-OH-MDZ-glucuronide and paraxanthine were monitored. These probe substances are specific substrates for CYP3A, CYP1A2 and P-glycoprotein. The

CL_{int} of midazolam, caffeine and digoxin thus reflect the activity of these proteins. In many investigations, the concentration ratio of the metabolites formed to the parent compound is used as a surrogate marker for the probe's CL_{int} (see for example references (57, 59, 60, 129)). The benefit of the method based on the concentration ratio is that the enzyme activity can be estimated with only one or two plasma samples. In this study, however, the collected data contained sufficient information to allow estimation of the pharmacokinetics of each compound using a population modelling approach, which is a more direct measurement of each CL_{int} value.

A Carbamazepine-Clomethiazole Interaction Model (Paper II)

All clomethiazole and NLA-715 data and the predictive performance of the final pharmacokinetic model are presented in Figure 5. The non-linear mixed effects modelling resulted in a three compartment model describing the pharmacokinetics of clomethiazole and a two compartment model describing the kinetics of NLA-715. Inter-individual variability was identified in the volume of distribution in the peripheral compartments, in the inter-compartmental clearance values, in $CL_{int\ CYPX}$, $CL_{int\ CYPY}$ and in the induction magnitude of $CL_{int\ CYPX}$ (IND_{CYPX}). The parameter estimates of all fixed and random effect parameters are presented in Table 1, with the corresponding relative standard errors from a 200 sample bootstrap.

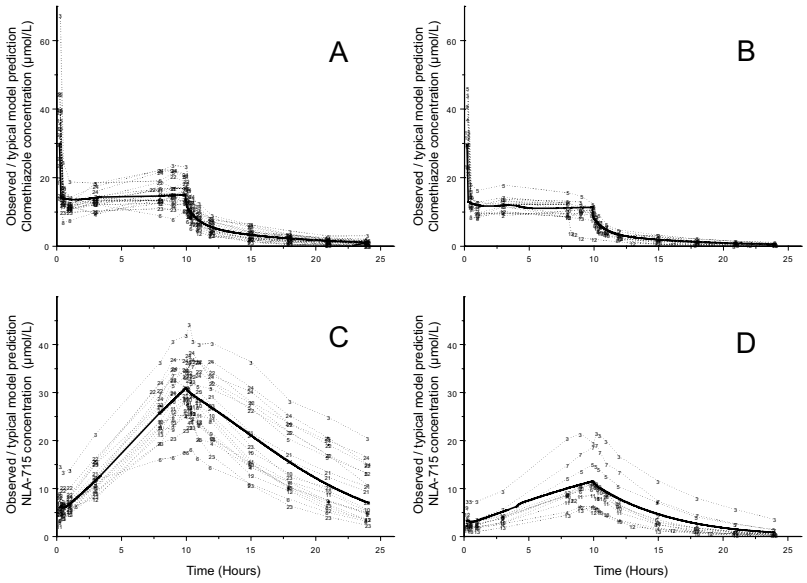

Figure 5 Dotted lines represent observed concentrations of clomethiazole before (A) and after (B) induction, and observed NLA-715 concentrations before (C) and after (D) induction. The solid lines represent the model predictions of a typical individual receiving the median clomethiazole dose.

Table 1 Parameter estimates with corresponding relative standard errors estimated by bootstrapping 200 datasets

Parameter	Estimate	RSE (%)	IIV	RSE (%)
$CL_{int\ CYPX}$ (L/h)	246	14.6	47.4	42.5
$CL_{int\ CYPY}$ (L/h)	70.3	15.5	23.6	31.8
$V_{max\ CYP2A6\text{-}CMZ}$ (µmol/h)	43.1	68.5	.	.
$K_{m\ CYP2A6\text{-}CMZ}$ (µmol/L)	0.778	24.0	.	.
$CL_{int\ CYP2A6\text{-}NLA}$ (L/h)	46.8	26.5	.	.
Induction $CL_{int\ CYPX}$ (%)	186	16.1	38.8	42.3
Induction $V_{max\ CYP2A6}$ (%)	81.7	11.6	.	.
$V_{C\ CMZ}$ (L)	5.0 (fix)	.	.	.
$V_{2\ CMZ}$ (L)	64.4	12.2	26.2	60.5
$V_{3\ CMZ}$ (L)	159	27.1	56.6	99.4
$V_{C\ NLA}$ (L)	5.0 (fix)	.	.	.
$V_{2\ NLA}$ (L)	43.9	14.4	15.7	56.5
$Q_{1\ CMZ}$ (L/h)	198	13.7	59.3	39.6
$Q_{2\ CMZ}$ (L/h)	64.4	12.6	26.5	60.0
$Q_{1\ NLA}$ (L/h)	31.8	17.7	21.2	47.7
Residual error CMZ (%)	15.0	6.43	.	.
Residual error NLA (%)	13.4	14.1	.	.
Residual error first observation (%)	23	16.3	.	.

CL_{int} = intrinsic clearance; V_{max} = maximal elimination rate; K_m = affinity constant; V_C = volume of the sampling compartment; $V_{2,3}$ = volume of the peripheral compartment; $Q_{1,2}$ = inter-compartment clearance

The mean concentration in the last clomethiazole sample drawn prior to the end of the infusion decreased from 15.8 µmol/L (range 10.2-23.2 µmol/L) to 9.69 µmol/L (6.14-12.3 µmol/L) as a result of the carbamazepine treatment. The NLA-715 concentrations increased linearly during the infusion, and reached a maximal concentration of 29.6 µmol/L (17.5-41.9 µmol/L) in the preinduced state, and 11.5 µmol/L (6.16-19.5 µmol/L) after induction. In the final model, $CL_{int\ CYPX}$ increased by 186%, and $V_{max\ CYP2A6\text{-}CMZ}$ and $V_{max\ CYP2A6\text{-}NLA}$ increased by 86% as a result of the carbamazepine treatment, while $CL_{int\ CYPY}$ was unaffected.

The initial peak concentration of clomethiazole is the result of the 15 minute loading infusion, and steady state conditions were thereafter rapidly met (Figure 5, a and b). The plasma concentration of NLA-715 increased in a linear manner during the infusion as opposed to the expected inverse exponential increase (Figure 5, c and d). Two approaches were evaluated to explain this phenomenon: a) a change in the blood flow to the liver, and b) non-linear kinetics, described below.

Clomethiazole has a high extraction ratio over the liver in the preinduced state, and the extraction ratio is further increased by enzyme induction. The clomethiazole systemic clearance has been found to be highly correlated to the blood flow to the liver (130), which is expected for a drug with such a high extraction ratio. In this study, food intake was prohibited from the night before the clomethiazole infusion. However, meals were served four hours after the start of the infusion. It has been reported that the blood flow to the liver increases by an average of 40% as a result of eating (116), so a 40% increase in the blood flow to the liver four hours after the start of the infusion was included in the model. The change in the blood flow resulted

in a significant drop in the objective function value, but had a limited impact on the models ability to predict the NLA-715 concentrations during the infusion, as seen in Figure 5, c and d. However, the change in the blood flow improved the fit of the clomethiazole data after carbamazepine treatment (Figure 5b). The clomethiazole plasma concentrations were lower after 8-10 hours than in the sample drawn at 3 hours, which is explained by the increased clomethiazole clearance, owing to the increased blood flow to the liver after eating food.

The second approach adopted to explain the linear increase in the NLA-715 concentration during the clomethiazole infusion was inspired by the Simcyp® simulations. These simulations predicted saturation in CYP2A6 at the experimental clomethiazole concentrations. Therefore, the elimination rate of NLA-715 was described by Equation 13c, as the saturable enzyme CYP2A6 is an important enzyme both in the formation and elimination of NLA-715. This non-linear model turned out to be the key to explaining the NLA-715 plasma concentration time profile. However, a normal non-linear model, where only the NLA-715 plasma concentrations cause non-linearity in $CL_{int\ CYP2A6\text{-}NLA}$ will result in a slow decline in the NLA-715 concentration after termination of the infusion, which does not agree with the experimental results (Figure 5d). However, rapidly declining NLA-715 concentrations could be achieved by applying a model with competitive metabolism of clomethiazole and NLA-715. When assuming such competitive behaviour, the $CL_{int\ CYP2A6\text{-}CMZ}$ and $CL_{int\ CYP2A6\text{-}NLA}$ are found to be dependent on both the clomethiazole and the NLA-715 concentrations (according to Equation 13c). Thereby, it was possible to explain the NLA-715 plasma concentration time profile. Our suggested explanation for this is that CYP2A6 has a high affinity, but low capacity (low K_m and low V_{max}) for clomethiazole, while CYP2A6 has a lower affinity to NLA-715. The consequence of this is negligible elimination of NLA-715 at high concentrations of clomethiazole, owing to the saturated CYP2A6 metabolism, resulting in a linear increase in the NLA-715 concentrations during the clomethiazole infusion. However, the clomethiazole concentrations decline rapidly as soon as the infusion is stopped. CYP2A6 is then no longer saturated, and NLA-715 can be eliminated with linear kinetics.

The early NLA-715 concentrations, drawn 30 minutes after the start of the infusion, decreased from 6.3 µmol/L (3.85-13.5 µmol/L) to 2.7 µmol/L (1.22-7.32 µmol/L). Negligible amounts of NLA-715 had been metabolised at this point in time. The decrease in the early NLA-715 plasma concentration is, therefore, probably the result of a change in the fraction of clomethiazole that is metabolised into NLA-715 (F_M). CYP3A4, which is an important enzyme in the formation NLA-715, is known to be induced by carbamazepine. However, alternative metabolic pathways for clomethiazole ($CL_{int\ CYPX}$) are likely to include both CYP3A4 and other CYP-isoenzymes that are inducible by carbamazepine. If these alternative metabolic pathways are induced to a higher extent than the one which leads to the production of NLA-715, a decrease in F_M would be expected. Indeed, the model suggested by this analysis predicts greater induction in these alternative metabolic pathways, than in the NLA-715 producing pathway, since the F_M was predicted to decrease from 17.6% to 7.34% as a result of carbamazepine treatment. However, the true F_M is close to unidentifiable without administering NLA-725 intravenously. The F_M estimated in this work is dependent on the fixed volume of the central compartments, and all NLA-715 pharmacokinetic parameters are relative to the true value of F_M.

In the protocol for the investigation, a doubling of the clomethiazole clearance

owing to carbamazepine-mediated induction was defined as being a clinically significant interaction. The clomethiazole clearance increased on average from 60 to 77 L/h, (before the meal was served) as a result of the carbamazepine treatment. This difference in clomethiazole clearance does not cause a significant interaction when clomethiazole is dosed intravenously. Such a change in clearance, however, might have a pronounced effect on the bioavailability of perorally dosed clomethiazole since the bioavailability is likely to be affected to a greater extent than the systemic clearance. A possible consequence of enzyme induction is an increased concentration of metabolites, which can result in toxicity. The NLA-715 exposure decreased drastically as a consequence of carbamazepine-mediated enzyme induction. In the model, this was explained as a combined result of increased NLA-715 metabolism and a change in the fraction of clomethiazole metabolised to NLA-715. It is, therefore, unlikely that the carbamazepine-clomethiazole interaction will cause toxicity related to NLA-715 exposure.

A model was presented describing the pharmacokinetics of clomethiazole and NLA-715 after administration of clomethiazole alone and after carbamazepine-mediated enzyme induction. Using a mechanistic approach, that is allowing changes in the blood flow to the liver, as a result of eating, and interpreting the *in vitro* generated metabolic information, a model was developed where the kinetics of clomethiazole and NLA-715 are described before and after enzyme induction. The NLA-715 plasma concentration time profile could not be explained using linear pharmacokinetic models. However, the developed model could explain these observations, and the underlying cause to the non-linearity in the pharmacokinetics of NLA-715 could be understood by combining enzyme activity measurements and a mechanistic pharmacokinetic model.

Pharmacodynamics of Enzyme Induction

Phenobarbital Induction in Rats (Paper III)

In Paper III, initially an empirical PB autoinduction model was developed, with an estimated half-life of the autoinduction process of 74 hours, with a 42 hour lag time for the onset of the induction. It was assumed that the delayed initiation of the induction was the result of the many steps necessary in the synthesis of new proteins and, therefore, similar lag times for the onset of the induction in the *in vitro* experiments were expected.

In the *in vitro* incubations, the PB treatment was found to increase the formation rates of 2β-, 6α-, 7α-, 16β-OHT, androstenedione and resorufin (see Figure 6). The time course of all induction processes appeared to be monoexponential, except the 7α-OHT induction, which formation rate increased linearly over time. All induction processes were modelled as being the result of an increased production rate (R_{in}) of the enzymes producing the probes, and the time course of the monoexponential inductions were described by turnover models (Equation 4) The half-life of the induction was estimated to 2 days for all processes except the androstenedione related induction, which was estimated to occur with a half-life of 3 days.

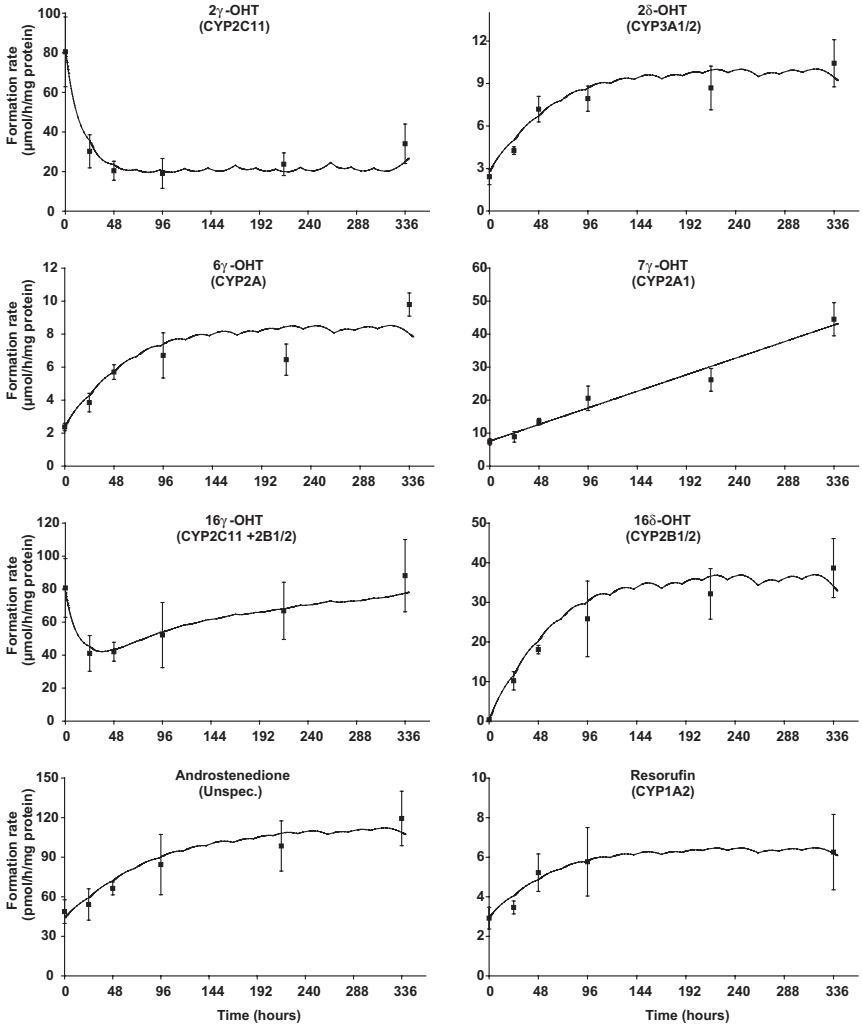

Figure 6 Filled squares represent observed average ± SD enzyme activity of each functional marker at each point in time. The solid line represent the model predicted formation rate of each functional markers.

The formation rates of 2α- and 16α-OHT declined as a consequence of the PB treatment. For 2α-OHT, this decrease in enzyme activity was modelled as an increase turnover rate (k_{out}) of the 2α-OHT producing enzyme. 16α-OHT is formed by the enzymes forming 2α-OHT and 16β-OHT, and thus, the changes in the 16α-OHT formation rate were modelled as a combination of the formation rates of 2α-OHT and 16β-OHT. Apparently, the time course of the induction process was much slower than the reduction in enzyme activity, which explains the initial decrease in the 16α-OHT formation rate.

No lag time for the onset of the induction was observed for any on the measured probes. However, by combining the rapid inhibition in the 2α-OHT production with the slow induction of the androstenedione producing enzymes, an enzyme

activity-time profile, which well mimicked the time profile of the empirical PB autoinduction model, could be obtained. Therefore, in the final model, PB affects the pharmacodynamics of eight of enzyme compartment, and two of these compartments then affected the elimination of PB (Figure 7 illustrates the structure of the final model). The pharmacokinetics of the autoinducing drug phenobarbital and its effect on a number of enzymes is thereby simultaneously described by integrating the bidirectional interaction between drug and enzymes in a mechanistic manner.

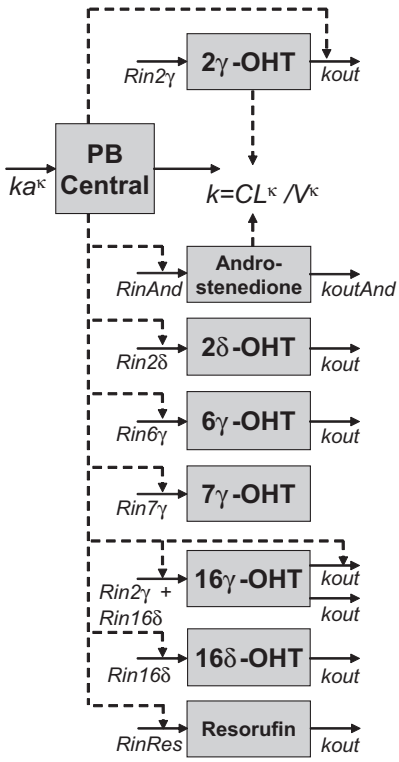

Figure 7 The structure of the final phenobarbital induction model. Filled arrows indicate production and elimination of enzymes, or absorption and elimination of phenobarbital. Dashed arrow indicates where the amount of one compartment increases the production or elimination of enzymes, or the phenobarbital clearance. η indicates where inter-individual variability was applied in the model.

Carbamazepine Induction in Man (Paper IV)

All measurements of the concentrations of carbamazepine and midazolam and the concentration-time profiles of caffeine and paraxanthine on days 1 and 16 are presented in Figure 8. The fixed and random effect parameters obtained from the final models are presented in Table 2 with their corresponding relative standard errors. The induction magnitudes were linearly correlated with the amount of inducing agents in all models (Equation 8). The time course of all induction processes was described with a turnover model (Equation 4).

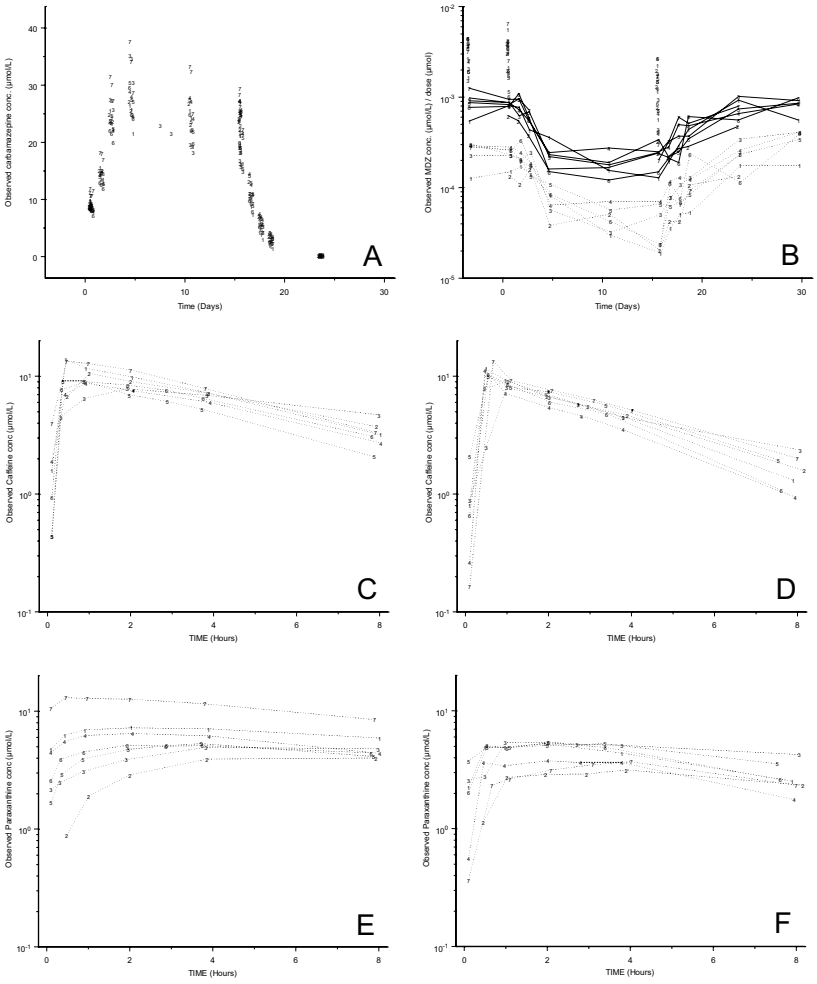

Figure 8 Observed concentrations of carbamazepine (A) and midazolam (B) versus time. The midazolam concentrations are dose adjusted. The numbers represent individual concentrations, the solid and dashed lines in panel B connects each individual's 4 and 8 hours samples respectively. Observed concentrations of caffeine on day 1 (C), caffeine on day 16 (D), paraxanthine on day 1 (E) and paraxanthine on day 16 (F) versus time.

The pharmacokinetics of digoxin were described using a two-compartment model, with inter-individual variability in the clearance, in the central volume of distribution and in the peripheral volume of distribution. The pharmacokinetcs of digoxin were unaffected by the carbamazepine treatment. This was quite surprising as it has been suggested that P-glycoprotein can be induced by CBZ (49). However, a recent *in vitro* study reported that CBZ does not alter the expression of P-glycoprotein (131), which is in agreement with our data.

Table 2 Parameter estimates with corresponding relative standard errors.

Parameter	Estimate	RSE (%)	IIV (%)	RSE (%)
Carbamazepine*				
CL_{CBZ1} → CBZ-E (L/h)	0.253	7.4	16.9	44
CL total, baseline (L/h)	1.27	.	.	.
V (L)	73.4	4.2	11.8	53
ka (h^{-1})	0.2 (fix)	.	.	.
Induction slope CL_{CBZ1} (%IND/µg CBZ+CBZ-E)	0.22	15.3	33.0	43
$t_{1/2}$ CBZ induction (h)	69.7	8.7	.	.
F 400mg CBZ (%)	83	2.5	.	.
Prop. residual error CBZ (%)	6.64	10.1	.	.
CBZ-E*				
CL (L/h)	5.82	10.7	12.8	61
V (L)	36.3	25.0	56.6	135
Induction slope CLCBZ-E (%IND/mg CBZ+CBZ-E)	0.39	79	.	.
$t_{1/2}$ CBZ-E induction (h)	1180	75	.	.
Prop. residual error CBZ-E (%)	9.14	12.9	.	.
Midazolam**				
CL hepatic, baseline(L/h)	38.9	3.3	6.2	58
V_1 (L)	84.4	5.2	.	.
V_2 (L)	41.4	25.3	16.1	56
Q (L/h)	9.24	22.6	12.	88
ka (h^{-1})	1.81	.	.	
Induction slope hepatic induction (%IND/µg CBZ+CBZ-E)	0.0462	19.5	5.1	60
$t_{1/2}$ hepatic induction (h)	69.7	8.9	.	.
Gut-wall extr. ratio, baseline (%)	43 (fix)	.	.	.
Induction slope gut-wall extr. ratio (%IND/µg CBZ+CBZ-E)	0.0847	31.5	.	.
$t_{1/2}$ gut-wall induction (h)	24 (fix)	.	.	.
Prop. residual error (%)	28.0	11.1	.	.
Digoxin*				
CL (L/h)	29.1	4.1	10	40
V_1 (L)	176	14	43	46
V_2 (L)	1060	7.3	15	48
Q (L/h)	111	6.6	.	.
ka (h^{-1})	1.45	9.9	.	.
IOV ka (%)	53	41	.	.
Prop. residual error (%)	21.6	7.5	.	.
Add. residual error (nmol/L)	0.0051	20	.	.
Caffeine**				
CL (L/h)	8.35	5.3	16	45
V (L)	41.7	6.8	14	45
ka (h^{-1})	4.24	.	.	.
IOV ka (%)	125	.	.	.
Induction slope CL (%IND/µg CBZ+CBZ-E)	0.0162	23	24	143
$t_{1/2}$ induction (h)	105	22	.	.
Paraxanthine**				
CL (L/h)	6.84	4.1	11	96
V (L)	32.9	3.1	.	.
Induction slope CL (%IND/µg CBZ+CBZ-E)	0.0272	17	32	115
$t_{1/2}$ induction (h)	105	22	.	.

* Modelling performed on plasma concentrations; ** Modelling performed on blood concentrations; CL = clearance; V and V_1 = volume of sampling compartment; V_2 = volume of peripheral compartment; ka = absorption rate constant; t½ induction = half-life of the induction; F = bioavailability; Q = inter-compartmental clearance; IOV = inter-occasion variability.

The final carbamazepine model consisted of one compartment for CBZ and one compartment for CBZ-E. The preinduced CBZ clearance was 1.3 L/h for a typical individual, increasing to 2.4 L/h after 16 days of CBZ treatment. The half-life of the CBZ autoinduction process was estimated to be 70 hours. The CBZ-E clearance increased, for a typical individual, from 5.8 L/h on day 1 to 13.6 L/h on day 16, with an estimated half-life for the CBZ-E induction of 1180 hours. Significant inter-individual variability was identified in the volume of the CBZ and CBZ-E compartments, in the preinduced clearances of CBZ and CBZ-E, and in the induction magnitude of CBZ.

The structure of the midazolam model, including a liver compartment, allowed a change in the hepatic metabolic clearance to simultaneously affect the bioavailability and systemic clearance of MDZ. However, by day 16 of the study, the level of induction in the systemic MDZ clearance was too low to fully explain the decreased MDZ exposure. CYP3A is the most abundant CYP-enzyme in the gut-wall mucosa (18), and MDZ is extensively metabolised when it is absorbed (119). Induction in the extraction ratio over the gut-wall will affect the bioavailability of a drug without changing the systemic elimination. Therefore, in an attempt to explain the more pronounced change in the bioavailability than in the systemic clearance, it was assumed that induction also affected the gut-wall extraction ratio. However, the days on which plasma samples only were drawn 4 and 8 hours after dose of the cocktail of drugs, provide limited information about the bioavailability of MDZ. It is, therefore difficult to accurately determine the time course of the CYP3A induction in the gut-wall mucosa. A half-life of the gut-wall epithelium of 24 hours has been reported (120), and therefore the half-life of the gut-wall induction was fixed to this value in the model. The extraction ratio over the gut-wall mucosa was 43% at baseline. The intrinsic clearance in the gut-wall was estimated to increase with 150% in the fully induced state, which resulted in a extraction ratio of 66%.

The half-life of the CYP3A liver induction was estimated to be 70 hours, which is in agreement with the time course of the CYP3A induction reported in other studies, which was review by Ghanbari et al. (132). The initial MDZ clearance was estimated to be 38 L/h. The hepatic CL_{int} had increased by 90% by the end of the CBZ treatment period, which resulted in a clearance of 54 L/h. Inter-individual variability was identified in the preinduced CL_{int}, in the peripheral volume of distribution, in the inter-compartmental clearance and in the induction magnitude in the liver.

In the CBZ sub-model, CYP3A was assumed to be the only inducible enzyme involved in the metabolism of CBZ. Moreover, it was assumed that the CYP3A metabolic pathway formed CBZ-E and that the fraction of CBZ metabolised into CBZ-E was 20% in the preinduced state. The inducible part of the CBZ clearance increased about 10 fold in the model, in an attempt to match the doubled CBZ clearance. However, the changes in the pharmacokinetics of midazolam predicted a doubled hepatic CYP3A-enzyme activity, owing to carbamazepine induction. Some of the assumptions made for the metabolism of CBZ are thus invalid. In order to make the magnitudes of the CBZ and MDZ induction match each other, other metabolic routes than the CBZ-E pathway could have been assumed to be inducible. This further illustrates the requirement for probe substances specifically metabolised by a certain CYP-enzyme in the development of enzyme induction models.

The caffeine sub-model consisted of one central compartment and one liver compartment for caffeine and paraxanthine, respectively. The caffeine CL_{int} increased

by 27% from the preinduced to the fully induced state, resulting in a change in clearance from 8.4 L/h to 10.4 L/h. The paraxanthine CL_{int} increased by 47% in response to the CBZ treatment, resulting in an increase in the paraxanthine clearance from 6.9 to 9.9 L/h. It was estimated that paraxanthine elimination was induced more strongly than the caffeine elimination. This is quite surprising, as both compounds are metabolised by CYP1A2 (133). However, other enzymes are involved in the metabolism of these compounds, and differences in the CYP-isoforms involved in these alternative metabolic routes could be an explanation for the difference in the induction magnitude. The half-life of the induction process was estimated to be 105 hours. Inter-individual variability was identified in the volume of the CAF compartment, in the clearances of CAF and PX and in the induction magnitude of CAF and PX.

In summary, the ability to model the pharmacodynamics of enzyme induction using a turnover model has been illustrated. Symmetrical induction models, with the same half-life of the induced enzymes during the onset of the induction and during its cessation, were obtained by including the pharmacokinetics of the inducing compound in the model. The half-life of induction in hepatic CYP3A was estimated to be 70 hours while the hepatic CYP1A2 had an induction half-life of 105 hours. This information can be of great value when designing interaction experiments, and important when making adjustments in doses after the initialization or termination of treatment with enzyme inducing compounds. To the best of our knowledge, this is the first model describing the pharmacodynamics of enzyme induction for specific CYP-enzymes in a controlled clinical trial.

Conclusions

In this thesis three key aspects of enzyme induction have been considered; the consequences for substrate elimination, the magnitude of the induction and the time course of the induction. Further, the incorporation of *in vitro* information as prior information for the *in vivo* situation has been demonstrated. New candidate drugs exhibiting enzyme inducing properties are often withdrawn from further drug development, due to the resulting complex pharmacokinetic characteristics and unwanted drug-drug interactions, which may be difficult to avoid despite restrictive drug labelling. The knowledge gained in this thesis contributes to a better understanding of the characteristics of enzyme induction. With this knowledge, the consequences of induction can be anticipated more easily, and the therapeutic risk related to induction can be reduced.

The consequences induction has on substrate elimination are stressed throughout this thesis. Paper II illustrated how existing *in vitro* information can be extrapolated to the *in vivo* situation, and be used to explain the pharmacokinetics of a metabolite. In this investigation, the plasma concentrations of a metabolite decreased as a result of the enzyme induction, in contrast to what would have been expected if no prior knowledge had existed of the metabolic disposition. In Paper III, isolated microsomes were incubated both with probe substrates and the metabolites that were formed during the incubations. The activity of the enzymes could be measured with better accuracy by including sequential metabolism in the *in vitro* experiments.

In three of the presented investigations the relationship between the plasma concentration of the inducer and the induction stimulus was described; as a step model in Paper II, as a linear function in Paper IV, and as an E_{max} model in Paper III. Of the three models applied, only the E_{max} model is physiologically plausible over a wide concentration range. To the best of our knowledge, the magnitude of the induction is only dependent on the characteristics of the inducing drug, i.e. it is a drug specific parameter. Therefore, the relationship between the plasma concentration of the inducer and the induction stimulus has to be established for every inducing agent and all enzymes affected. However, the maximum induction magnitude might be a system specific parameter, which for example, could be determined by the maximal transcription rate of the genome. If this is the case, the E_{max} parameter of a specific enzyme could, once estimated, be used as an initial value in further induction investigations.

The time course of the induction process was estimated in this thesis. In Paper III, the turnover rates of several enzymes were estimated, using *in vitro* techniques for the enzyme activity measurement. In Paper IV, the turnover rates of CYP3A and CYP1A2 were estimated in healthy volunteers by dosing them with a cocktail of

CYP-probes. The turnover rate of the induced enzyme is a system specific parameter, which together with the kinetic properties of the inducer, determines the time course of the induction. Hence, the estimated turnover rates of the CYP-enzymes can be of great value as the input in future induction models, thereby making it possible to predict the elimination rate of a compound at any point in time during the induction process.

Another aspect of the induction time course, the delayed onset of the induction, was evaluated in two investigations. In Paper III, a 48 hour time lag before the onset of the phenobarbital autoinduction was observed. However, this was not reflected in the metabolic activity for any of the enzymes. Instead, the apparent lag time was explained as the result of a rapid phenobarbital-mediated enzyme inhibition, followed by a slower induction process. In Paper IV, no significant delay was noted before the commencement of carbamazepine-mediated induction of CYP3A and CYP1A2.

Knowledge of the time course of enzyme induction can be of great importance for drug development and in clinical practice. Our results suggest that, for an enzyme inducer that does not simultaneously act as a CYP-inhibitor, 50% of the maximal induction is attained within a few days of the start of the treatment, and that 90% of the fully induced enzyme level is attained after about 10-14 days, for induction of CYP3A and CYP2A1.

Several investigations can be thought of to further improve the understanding of all aspects of the induction process. It would be of great interest to investigate the relationship between the induction stimulus and the plasma concentration of the inducer in greater depth. An estimation of the turnover rate of other important CYP-enzymes in the liver and in extra hepatic tissues would also be valuable. With a good understanding of the magnitude of the induction and the turnover rate of the enzymes in the relevant tissues, the consequences of the induction process could be better predicted. Moreover, by estimating these parameters in a larger population, the inter-individual variability could be assessed.

Mats Magnusson

Populärvetenskaplig sammanfattning

Vi utsätts dagligen för en stor mängd främmande ämnen. Dessa ämnen kan, om de ansamlas i höga halter, skada kroppen. Människan har därför utvecklat passiva och aktiva försvarsmekanismer mot dessa ämnen. Det passiva försvaret utgörs främst av barriärer, så som huden och täta blodkärl i särskilt känsliga organ. Det aktiva försvaret består av proteiner, dels i form av enzymer, dels i form av transportprotein. Enzymer har till uppgift att göra de främmande ämnena mer vattenlösliga, vilket i sin tur gör det möjligt för kroppen att göra sig av med ämnet. Transportproteinerna fungerar som pumpar som förhindrar ämnen från att ta sig in i kroppen, eller pumpar ut ämnen som redan absorberats. Då kroppen utsätts för vissa främmande ämnen ökar tillverkningen av dessa protein. Detta kallas induktion, och kan antas vara ytterligare ett sätt för kroppen att skydda sig från skadliga ämnen. Exempel på ämnen som kan ge upphov till induktion är cigarettrök, alkohol, vissa miljögifter och läkemedel. Inom läkemedelsutvecklingen är det viktigt att studera förekomst av enzyminduktion. Induktionen kan leda till att mängden läkemedel sjunker i kroppen, vilket får till följd att läkemedlets effekt försämras eller uteblir.

Målet med detta avhandlingsarbete har varit att studera induktionen av framförallt enzymer, men även till viss del transportproteiner. I det första delarbetet utvecklades en kemisk analysmetod som gör det möjligt att bestämma med vilken hastighet testosterons nedbrytningsprodukter bildas. Genom att i ett provrör blanda testosteron med renframställda enzymer, och därefter mäta hur snabbt vissa nedbrytningsprodukter bildas, erhålls ett mått på enzymmängden i provet.

Enzyminduktion leder till att kroppen snabbare gör sig av med läkemedel. Det finns också risk för att mängden av nedbrytningsprodukter ökar, till följd av induktionen, vilket kan skada kroppen. I det andra delarbetet studerades hur det enzyminducerande läkemedlet karbamazepin påverkar nedbrytningen av läkemedlet clometiazol, och hur det påverkade mängden av clometiazols nedbrytningsprodukt, NLA-715. I studien gavs clometiazol till 16 försökspersoner före och efter en tvåveckors behandling med karbamazepin. Mängden clometiazol sjönk, som väntat, till följd av enzyminduktionen. Ett oväntat resultat var att även mängden NLA-715 gick ner. Dessutom förändrades mängden NLA-715 i kroppen på en svårförklarlig sätt, under och efter doseringen med clometiazol. För att förklara de oväntade resultaten togs hjälp av tidigare experiment, då det undersökts vilka enzymer som bidrar till clometiazols och NLA-715's nedbrytning. Genom att bygga in denna information i en modell kunde de oväntade resultaten förklaras.

I det tredje delarbetet gavs det enzyminducerande läkemedlet fenobarbital till råttor, i upp till två veckor. Fenobarbital påverkar många enzymer, inklusive de enzymer som bryter ner fenobarbital självt. Mängden fenobarbital i råttornas blod mättes varje dag, och mängden enzymer kunde, med den metod som utvecklats i det första delarbetet, bestämmas vid olika tidpunkter under induktionsförloppet. Utifrån dessa data skapades en modell som beskriver tidsförloppet för induktionen av flera

enzymer i råttornas lever.

Målet med det fjärde delarbetet var att studera tidsförloppet för enzyminduktion i människa. Denna studie likar på så sätt delarbete tre. Enzymmängden bestämdes genom att blodprover togs från sju frivilliga försökspersoner som fått ett läkemedel som bryts ner av vissa enzymer. Genom att beräkna med vilken hastighet kroppen gjorde sig av med läkemedlen kunde mängden av dessa enzym bestämmas innan, under och efter behandling med karbamazepin. Det kan antas att graden av induktion är beroende av hur stor mängd av det inducerande ämnet som kroppen utsätts för, medan tidsförloppet för induktionen i hög grad bestäms av det påverkade proteinets omsättningshastighet. Med dessa antaganden utvecklades en modell som beskriver storleken och tidsförloppet för induktionen av två enzymer.

Sammanfattningsvis kan sägas att detta avhandlingsarbete ökat förståelsen för hur inducerande läkemedel påverkar enzymer som bryter ner läkemedel. Denna kunskap kan få betydelse för hur induktionsstudier genomförs i läkemedelsindustrin och för hur och när dosen av vissa läkemedel justeras när en patient inleder eller avslutar en behandling med ett enzyminducerande läkemedel.

Liten ordlista

Pharmacokinetics	- vad kroppen gör med läkemedel
Pharmacodynamics	- vad läkemedlet gör med kroppen
CYP = cytochrome P450	- en grupp läkemedelsnedbrytande enzymer
P-gp = P-glycoprotein	- ett transportprotein
NONMEM	- resultaten har utvärderats med detta program

Acknowledgements

The work presented in this thesis was carried out at the Department of Pharmaceutical Biosciences, Division of Pharmacokinetics and Drug Therapy, Faculty of Pharmacy, Uppsala University, Sweden.

I would like to express my sincere gratitude to all who have contributed to this thesis and especially to:

Min handledare, dr Rikard Sandström, för vetenskaplig handledning. Tack för att du antog mig som doktorand, och för att du givit mig stor frihet i val av forskningens inriktning. Tack också för alla resor och alla roliga stunder vi haft.

Min biträdande handledare, professor Mats O Karlsson, för alla förträffliga tankar du bidragit med. Tack också för att du, trots ditt pressade tidschema, månar om alla doktorander på avdelningen.

Professor Margareta Hammarlund-Udenaes, för att du är en utmärkt chef för avdelningen, som emellanåt får oss doktorander att lyfta blicken och se att det vi gör är bra.

Professor Emeritus Lennart Paalzow och dr Marie Sandström för att ni från början fick mig intresserad av farmakokinetisk forskning.

Mina medförfattare till klomethiazol-arbetet, dr Per-Henrik Zingmark och dr Bo Fransson, för att ni genomförde denna studie, och för att ni lät mig modellera de data som genererats. Stort tack även till Ann-Louise Hagbjörk och Karl-Gustav Jostell för värdefull hjälp med detta arbete.

Mina medförfattare till cocktail-arbetet, professor Marja-Liisa Dahl och dr Jonas Cederberg, för att ni möjliggjorde denna studie, och att ni genomförde den så väl. Särskilt tack för att ni varit så engagerade och för all hjälp med ansökningshandlingar och protokoll. Stort tack även till Inga-Lena Sporrong för utmärkt provtagning, och till de friska försökspersonerna som frivilligt deltog i denna studie.

Britt Jansson, Magnus Jansson, Jessica Strömgren och Kjell Berggren för utmärkt teknisk hjälp.

Min promotor, min strukturerare, min korrekturläsare och min extra handledare, dr Siv Jönsson. Utan din hjälp hade ingen begripit vad som står i den här avhandlingen, nu vet jag i alla fall att en person förstått. Tack för att du alltid har tagit dig tid att hjälpa mig oavsett vilken typ av problem jag haft.

Min rumskompis, och andra extra handledare, dr Lars Lindbom. Tack för att du dagligen hjälpt mig med små och stora saker. Tänk vad mycket du kommer få uträttat när jag nu slutar störa dig.

Mina exjobbare: Karolina Rosquist, Frida Sjöberg, Veronica Svahn, Petra Bjärenstam, Anders Wallin, Malin Justrell och Erik Sjögren. Tack för er värdefulla insats, tack, tack och tack igen.

Dr Niclas Jonsson för att du utvecklat Xpose, som jag haft mycket glädje av, och för att du låtit mig vinna dom flesta badmintonmatcherna.

Pontus Pihlgren, för oumbärlig hjälp med klustret.

Alla nuvarande och tidigare kollegor på avdelningen, jag minns er alla med glädje.

Till mina vänner och min familj:

Jakob, dr Olle, Tobbe och Micke. Tack grabbar för alla trevliga seglingar och andra äventyr.

Karin, min bästa tjejkompis, och Anna, Matilda, Anna och Sofia, som också är det.

Pär och Finkan, för att ni är så goa.

Sigrid, Ida, Love, Elis, Idun, Erland, Morgan, Jakob, Sofia, Ellen och era föräldrar.

Alla som avnjuter vin lika Verdamt som jag själv.

Skökan, Lybban och Mackan för skojiga spelkvällar

Alla fastrar, farbröder, mostrar och morbröder, kusiner och sysslingar.

Barbro, Yngve, Mia, Stefan och Viktor, för att Flugdammen aldrig känns långt borta.

Måns, Mikaela och Sixten. Den bästa bror man kan ha, med bästa tänkbara svägerska och barn.

Petter, Frida, Dante och Katla. Den bästa bror man kan ha, med bästa tänkbara svägerska och barn.

Klara, Olle och Anton, ni är också bra.

Pappa, min första förebild i forskarvärlden, avhandlingen blev kanske inte så bra som din, men jag tror att den duger.

Mamma, först, tack för all praktisk hjälp under avhandlingsarbetet. Tack också för att du är den bästa mamma man kan växa upp med, och för att du alltid med en självklarhet utgått från att allt jag företar mig kommer slutföras med största möjliga framgång.

Oscar, tänk att jag under mer än 30 år inte träffat någon person som ger mig så mycket glädje, och som ger mitt liv en sådan mening som du Oscar. Du är helt fantastisk.

Kommande syskon till Oscar, ni kommer bli lika viktiga för mig som er storebror.

Monika, för att du är mitt livs kärlek och för att varje dag med dig är fenomenal. Jag älskar dig alltid.

References

1. Conney AH, Davison C, Gastel R, Burns JJ. Adaptive increases in drug-metabolizing enzymes induced by phenobarbital and other drugs. J Pharmacol Exp Ther. 1960 Sep;130:1-8.
2. Conney AH, Gillette JR, Inscoe JK, Trams ER, Posner HS. Induced synthesis of liver microsomal enzymes which metabolize foreign compounds. Science. 1959 Nov 27;130:1478-9.
3. Luo G, Cunningham M, Kim S, Burn T, Lin J, Sinz M, et al. CYP3A4 induction by drugs: correlation between a pregnane X receptor reporter gene assay and CYP3A4 expression in human hepatocytes. Drug Metab Dispos. 2002 Jul;30(7):795-804.
4. Yeh RF, Gaver VE, Patterson KB, Rezk NL, Baxter-Meheux F, Blake MJ, et al. Lopinavir/ritonavir induces the hepatic activity of cytochrome P450 enzymes CYP2C9, CYP2C19, and CYP1A2 but inhibits the hepatic and intestinal activity of CYP3A as measured by a phenotyping drug cocktail in healthy volunteers. J Acquir Immune Defic Syndr. 2006 May;42(1):52-60.
5. Christensen M, Andersson K, Dalen P, Mirghani RA, Muirhead GJ, Nordmark A, et al. The Karolinska cocktail for phenotyping of five human cytochrome P450 enzymes. Clin Pharmacol Ther. 2003 Jun;73(6):517-28.
6. Frye RF, Matzke GR, Adedoyin A, Porter JA, Branch RA. Validation of the five-drug "Pittsburgh cocktail" approach for assessment of selective regulation of drug-metabolizing enzymes. Clin Pharmacol Ther. 1997 Oct;62(4):365-76.
7. Branch RA, Adedoyin A, Frye RF, Wilson JW, Romkes M. In vivo modulation of CYP enzymes by quinidine and rifampin. Clin Pharmacol Ther. 2000 Oct;68(4):401-11.
8. Garfinkel D. Studies on pig liver microsomes. I. Enzymic and pigment composition of different microsomal fractions. Arch Biochem Biophys. 1958 Oct;77(2):493-509.
9. Klingenberg M. Pigments of rat liver microsomes. Arch Biochem Biophys. 1958;75(2):376-86.
10. Omura T, Sato R. A new cytochrome in liver microsomes. J Biol Chem. 1962 Apr;237:1375-6.
11. Omura T, Sato R. The Carbon Monoxide-Binding Pigment of Liver Microsomes. I. Evidence for Its Hemoprotein Nature. J Biol Chem. 1964 Jul;239:2370-8.
12. Cooper DY, Levin S, Narasimhulu S, Rosenthal O. Photochemical Action Spectrum of the Terminal Oxidase of Mixed Function Oxidase Systems. Science. 1965 Jan 22;147:400-2.
13. Estabrook RW, Cooper DY, Rosenthal O. The Light Reversible Carbon Monoxide Inhibition of the Steroid C21-Hydroxylase System of the Adrenal Cortex. Biochem Z. 1963;338:741-55.
14. Krishna DR, Klotz U. Extrahepatic metabolism of drugs in humans. Clin Pharmacokinet. 1994 Feb;26(2):144-60.
15. Lin JH, Lu AY. Interindividual variability in inhibition and induction of cytochrome P450 enzymes. Annu Rev Pharmacol Toxicol. 2001;41:535-67.
16. Wilkinson GR. Drug metabolism and variability among patients in drug response. N Engl J Med. 2005 May 26;352(21):2211-21.

17. Fromm MF, Busse D, Kroemer HK, Eichelbaum M. Differential induction of prehepatic and hepatic metabolism of verapamil by rifampin. Hepatology. 1996 Oct;24(4):796-801.
18. Paine MF, Hart HL, Ludington SS, Haining RL, Rettie AE, Zeldin DC. The human intestinal cytochrome P450 "pie". Drug Metab Dispos. 2006 May;34(5):880-6.
19. Zamek-Gliszczynski MJ, Hoffmaster KA, Nezasa K, Tallman MN, Brouwer KL. Integration of hepatic drug transporters and phase II metabolizing enzymes: mechanisms of hepatic excretion of sulfate, glucuronide, and glutathione metabolites. Eur J Pharm Sci. 2006 Apr;27(5):447-86.
20. Juliano RL, Ling V. A surface glycoprotein modulating drug permeability in Chinese hamster ovary cell mutants. Biochim Biophys Acta. 1976 Nov 11;455(1):152-62.
21. Fojo AT, Ueda K, Slamon DJ, Poplack DG, Gottesman MM, Pastan I. Expression of a multidrug-resistance gene in human tumors and tissues. Proc Natl Acad Sci U S A. 1987 Jan;84(1):265-9.
22. Thiebaut F, Tsuruo T, Hamada H, Gottesman MM, Pastan I, Willingham MC. Cellular localization of the multidrug-resistance gene product P-glycoprotein in normal human tissues. Proc Natl Acad Sci U S A. 1987 Nov;84(21):7735-8.
23. Cordon-Cardo C, O'Brien JP, Boccia J, Casals D, Bertino JR, Melamed MR. Expression of the multidrug resistance gene product (P-glycoprotein) in human normal and tumor tissues. J Histochem Cytochem. 1990 Sep;38(9):1277-87.
24. Cordon-Cardo C, O'Brien JP, Casals D, Rittman-Grauer L, Biedler JL, Melamed MR, et al. Multidrug-resistance gene (P-glycoprotein) is expressed by endothelial cells at blood-brain barrier sites. Proc Natl Acad Sci U S A. 1989 Jan;86(2):695-8.
25. Borst P, Elferink RO. Mammalian ABC transporters in health and disease. Annu Rev Biochem. 2002;71:537-92.
26. Wacher VJ, Wu CY, Benet LZ. Overlapping substrate specificities and tissue distribution of cytochrome P450 3A and P-glycoprotein: implications for drug delivery and activity in cancer chemotherapy. Mol Carcinog. 1995 Jul;13(3):129-34.
27. Scott RJ, Palmer J, Lewis IA, Pleasance S. Determination of a 'GW cocktail' of cytochrome P450 probe substrates and their metabolites in plasma and urine using automated solid phase extraction and fast gradient liquid chromatography tandem mass spectrometry. Rapid Commun Mass Spectrom. 1999;13(23):2305-19.
28. Levy RH, Lai AA, Dumain MS. Time-dependent kinetics IV: Pharmacokinetic theory of enzyme induction. J Pharm Sci. 1979 Mar;68(3):398-9.
29. Okey AB. Enzyme induction in the cytochrome P-450 system. Pharmacol Ther. 1990;45(2):241-98.
30. Handschin C, Meyer UA. Induction of drug metabolism: the role of nuclear receptors. Pharmacol Rev. 2003 Dec;55(4):649-73.
31. Song BJ, Matsunaga T, Hardwick JP, Park SS, Veech RL, Yang CS, et al. Stabilization of cytochrome P450j messenger ribonucleic acid in the diabetic rat. Mol Endocrinol. 1987 Aug;1(8):542-7.
32. Chien JY, Thummel KE, Slattery JT. Pharmacokinetic consequences of induction of CYP2E1 by ligand stabilization. Drug Metab Dispos. 1997 Oct;25(10):1165-75.
33. Gonzalez FJ, Fernandez-Salguero P. The aryl hydrocarbon receptor: studies using the AHR-null mice. Drug Metab Dispos. 1998 Dec;26(12):1194-8.
34. Li W, Harper PA, Tang BK, Okey AB. Regulation of cytochrome P450 enzymes by aryl hydrocarbon receptor in human cells: CYP1A2 expression in the LS180 colon carcinoma cell line after treatment with 2,3,7,8-tetrachlorodibenzo-p-dioxin or 3-methylcholanthrene. Biochem Pharmacol. 1998 Sep 1;56(5):599-612.
35. Faber MS, Fuhr U. Time response of cytochrome P450 1A2 activity on cessation of heavy smoking. Clin Pharmacol Ther. 2004 Aug;76(2):178-84.

36. Baes M, Gulick T, Choi HS, Martinoli MG, Simha D, Moore DD. A new orphan member of the nuclear hormone receptor superfamily that interacts with a subset of retinoic acid response elements. Mol Cell Biol. 1994 Mar;14(3):1544-52.
37. Bertilsson G, Heidrich J, Svensson K, Asman M, Jendeberg L, Sydow-Backman M, et al. Identification of a human nuclear receptor defines a new signaling pathway for CYP3A induction. Proc Natl Acad Sci U S A. 1998 Oct 13;95(21):12208-13.
38. Wei P, Zhang J, Egan-Hafley M, Liang S, Moore DD. The nuclear receptor CAR mediates specific xenobiotic induction of drug metabolism. Nature. 2000 Oct 19;407(6806):920-3.
39. Faucette SR, Zhang TC, Moore R, Sueyoshi T, Omiecinski CJ, LeCluyse EL, et al. Relative activation of human pregnane X receptor versus constitutive androstane receptor defines distinct classes of CYP2B6 and CYP3A4 inducers. J Pharmacol Exp Ther. 2007 Jan;320(1):72-80.
40. Synold TW, Dussault I, Forman BM. The orphan nuclear receptor SXR coordinately regulates drug metabolism and efflux. Nat Med. 2001 May;7(5):584-90.
41. Pang KS, Rowland M. Hepatic clearance of drugs. I. Theoretical considerations of a "well-stirred" model and a "parallel tube" model. Influence of hepatic blood flow, plasma and blood cell binding, and the hepatocellular enzymatic activity on hepatic drug clearance. J Pharmacokinet Biopharm. 1977 Dec;5(6):625-53.
42. Pang KS, Rowland M. Hepatic clearance of drugs. II. Experimental evidence for acceptance of the "well-stirred" model over the "parallel tube" model using lidocaine in the perfused rat liver in situ preparation. J Pharmacokinet Biopharm. 1977 Dec;5(6):655-80.
43. Pang KS, Rowland M. Hepatic clearance of drugs. III. Additional experimental evidence supporting the "well-stirred" model, using metabolite (MEGX) generated from lidocaine under varying hepatic blood flow rates and linear conditions in the perfused rat liver in situ preparation. J Pharmacokinet Biopharm. 1977 Dec;5(6):681-99.
44. Paine MF, Shen DD, Kunze KL, Perkins JD, Marsh CL, McVicar JP, et al. First-pass metabolism of midazolam by the human intestine. Clin Pharmacol Ther. 1996 Jul;60(1):14-24.
45. Wang Z, Gorski JC, Hamman MA, Huang SM, Lesko LJ, Hall SD. The effects of St John's wort (Hypericum perforatum) on human cytochrome P450 activity. Clin Pharmacol Ther. 2001 Oct;70(4):317-26.
46. Alvan G, Piafsky K, Lind M, von Bahr C. Effect of pentobarbital on the disposition of alprenolol. Clin Pharmacol Ther. 1977 Sep;22(3):316-21.
47. von Bahr C, Steiner E, Koike Y, Gabrielsson J. Time course of enzyme induction in humans: effect of pentobarbital on nortriptyline metabolism. Clin Pharmacol Ther. 1998 Jul;64(1):18-26.
48. Greiner B, Eichelbaum M, Fritz P, Kreichgauer HP, von Richter O, Zundler J, et al. The role of intestinal P-glycoprotein in the interaction of digoxin and rifampin. J Clin Invest. 1999 Jul;104(2):147-53.
49. Giessmann T, May K, Modess C, Wegner D, Hecker U, Zschiesche M, et al. Carbamazepine regulates intestinal P-glycoprotein and multidrug resistance protein MRP2 and influences disposition of talinolol in humans. Clin Pharmacol Ther. 2004 Sep;76(3):192-200.
50. Bjornsson TD, Callaghan JT, Einolf HJ, Fischer V, Gan L, Grimm S, et al. The conduct of in vitro and in vivo drug-drug interaction studies: a Pharmaceutical Research and Manufacturers of America (PhRMA) perspective. Drug Metab Dispos. 2003 Jul;31(7):815-32.
51. Tucker GT, Houston JB, Huang SM. Optimizing drug development: strategies to assess drug metabolism/transporter interaction potential--toward a consensus. Pharm Res. 2001 Aug;18(8):1071-80.
52. Obach RS, Baxter JG, Liston TE, Silber BM, Jones BC, MacIntyre F, et al. The prediction of human pharmacokinetic parameters from preclinical and in vitro metabolism data. J Pharmacol Exp Ther. 1997 Oct;283(1):46-58.

53. Obach RS. Prediction of human clearance of twenty-nine drugs from hepatic microsomal intrinsic clearance data: An examination of in vitro half-life approach and nonspecific binding to microsomes. Drug Metab Dispos. 1999 Nov;27(11):1350-9.
54. Burnette WN. "Western blotting": electrophoretic transfer of proteins from sodium dodecyl sulfate--polyacrylamide gels to unmodified nitrocellulose and radiographic detection with antibody and radioiodinated protein A. Anal Biochem. 1981 Apr;112(2):195-203.
55. Wang AM, Doyle MV, Mark DF. Quantitation of mRNA by the polymerase chain reaction. Proc Natl Acad Sci U S A. 1989 Dec;86(24):9717-21.
56. Wong H, Anderson WD, Cheng T, Riabowol KT. Monitoring mRNA expression by polymerase chain reaction: the "primer-dropping" method. Anal Biochem. 1994 Dec;223(2):251-8.
57. Thummel KE, Shen DD, Podoll TD, Kunze KL, Trager WF, Bacchi CE, et al. Use of midazolam as a human cytochrome P450 3A probe: II. Characterization of inter- and intraindividual hepatic CYP3A variability after liver transplantation. J Pharmacol Exp Ther. 1994 Oct;271(1):557-66.
58. Kirby B, Kharasch ED, Thummel KT, Narang VS, Hoffer CJ, Unadkat JD. Simultaneous measurement of in vivo P-glycoprotein and cytochrome P450 3A activities. J Clin Pharmacol. 2006 Nov;46(11):1313-9.
59. Rostami-Hodjegan A, Nurminen S, Jackson PR, Tucker GT. Caffeine urinary metabolite ratios as markers of enzyme activity: a theoretical assessment. Pharmacogenetics. 1996 Apr;6(2):121-49.
60. Carrillo JA, Christensen M, Ramos SI, Alm C, Dahl ML, Benitez J, et al. Evaluation of caffeine as an in vivo probe for CYP1A2 using measurements in plasma, saliva, and urine. Ther Drug Monit. 2000 Aug;22(4):409-17.
61. Howgate EM, Rowland Yeo K, Proctor NJ, Tucker GT, Rostami-Hodjegan A. Prediction of in vivo drug clearance from in vitro data. I: impact of inter-individual variability. Xenobiotica. 2006 Jun;36(6):473-97.
62. Rostami-Hodjegan A, Tucker GT. Simulation and prediction of in vivo drug metabolism in human populations from in vitro data. Nat Rev Drug Discov. 2007 Feb;6(2):140-8.
63. Garlick PJ, Waterlow JC, Swick RW. Measurement of protein turnover in rat liver. Analysis of the complex curve for decay of label in a mixture of proteins. Biochem J. 1976 Jun 15;156(3):657-63.
64. Lai AA, Levy RH, Cutler RE. Time-course of interaction between carbamazepine and clonazepam in normal man. Clin Pharmacol Ther. 1978 Sep;24(3):316-23.
65. Dayneka NL, Garg V, Jusko WJ. Comparison of four basic models of indirect pharmacodynamic responses. J Pharmacokinet Biopharm. 1993 Aug;21(4):457-78.
66. Kliewer SA, Moore JT, Wade L, Staudinger JL, Watson MA, Jones SA, et al. An orphan nuclear receptor activated by pregnanes defines a novel steroid signaling pathway. Cell. 1998 Jan 9;92(1):73-82.
67. Renwick AB, Watts PS, Edwards RJ, Barton PT, Guyonnet I, Price RJ, et al. Differential maintenance of cytochrome P450 enzymes in cultured precision-cut human liver slices. Drug Metab Dispos. 2000 Oct;28(10):1202-9.
68. Rostami-Hodjegan A, Wolff K, Hay AW, Raistrick D, Calvert R, Tucker GT. Population pharmacokinetics of methadone in opiate users: characterization of time-dependent changes. Br J Clin Pharmacol. 1999 Jul;48(1):43-52.
69. Hsu A, Granneman GR, Witt G, Locke C, Denissen J, Molla A, et al. Multiple-dose pharmacokinetics of ritonavir in human immunodeficiency virus-infected subjects. Antimicrob Agents Chemother. 1997 May;41(5):898-905.
70. Ariens EJ, Simonis AM. A Molecular Basis for Drug Action. the Interaction of One or More Drugs with Different Receptors. J Pharm Pharmacol. 1964 May;16:289-312.
71. Ehrnebo M. Pharmacokinetics and distribution properties of pentobarbital in humans following oral and intravenous administration. J Pharm Sci. 1974 Jul;63(7):1114-8.

72. Hassan M, Svensson US, Ljungman P, Bjorkstrand B, Olsson H, Bielenstein M, et al. A mechanism-based pharmacokinetic-enzyme model for cyclophosphamide autoinduction in breast cancer patients. Br J Clin Pharmacol. 1999 Nov;48(5):669-77.
73. Kerbusch T, Huitema AD, Ouwerkerk J, Keizer HJ, Mathot RA, Schellens JH, et al. Evaluation of the autoinduction of ifosfamide metabolism by a population pharmacokinetic approach using NONMEM. Br J Clin Pharmacol. 2000 Jun;49(6):555-61.
74. Kahn MG, Fagan LM, Sheiner LB. Combining physiologic models and symbolic methods to interpret time-varying patient data. Methods Inf Med. 1991 Aug;30(3):167-78.
75. Sun YN, Jusko WJ. Transit compartments versus gamma distribution function to model signal transduction processes in pharmacodynamics. J Pharm Sci. 1998 Jun;87(6):732-7.
76. Frame B, Beal SL. Non-steady state population kinetics of intravenous phenytoin. Ther Drug Monit. 1998 Aug;20(4):408-16.
77. Boddy AV, Cole M, Pearson AD, Idle JR. The kinetics of the auto-induction of ifosfamide metabolism during continuous infusion. Cancer Chemother Pharmacol. 1995;36(1):53-60.
78. Gordi T, Xie R, Huong NV, Huong DX, Karlsson MO, Ashton M. A semiphysiological pharmacokinetic model for artemisinin in healthy subjects incorporating autoinduction of metabolism and saturable first-pass hepatic extraction. Br J Clin Pharmacol. 2005 Feb;59(2):189-98.
79. Chang TK, Yu L, Maurel P, Waxman DJ. Enhanced cyclophosphamide and ifosfamide activation in primary human hepatocyte cultures: response to cytochrome P-450 inducers and autoinduction by oxazaphosphorines. Cancer Res. 1997 May 15;57(10):1946-54.
80. Kostrubsky VE, Ramachandran V, Venkataramanan R, Dorko K, Esplen JE, Zhang S, et al. The use of human hepatocyte cultures to study the induction of cytochrome P-450. Drug Metab Dispos. 1999 Aug;27(8):887-94.
81. Abramson FP. Kinetic models of induction: I. Persistence of the inducing substance. J Pharm Sci. 1986 Mar;75(3):223-8.
82. Sheiner L, Wakefield J. Population modelling in drug development. Stat Methods Med Res. 1999 Sep;8(3):183-93.
83. Marshall S, Macintyre F, James I, Krams M, Jonsson NE. Role of mechanistically-based pharmacokinetic/pharmacodynamic models in drug development : a case study of a therapeutic protein. Clin Pharmacokinet. 2006;45(2):177-97.
84. Nestorov IS, Hadjitodorov ST, Petrov I, Rowland M. Empirical versus mechanistic modelling: comparison of an artificial neural network to a mechanistically based model for quantitative structure pharmacokinetic relationships of a homologous series of barbiturates. AAPS PharmSci. 1999;1(4):E17.
85. Friberg LE, Karlsson MO. Mechanistic models for myelosuppression. Invest New Drugs. 2003 May;21(2):183-94.
86. Sheiner LB, Beal SL. Evaluation of methods for estimating population pharmacokinetics parameters. I. Michaelis-Menten model: routine clinical pharmacokinetic data. J Pharmacokinet Biopharm. 1980 Dec;8(6):553-71.
87. Sheiner LB. The population approach to pharmacokinetic data analysis: rationale and standard data analysis methods. Drug Metab Rev. 1984;15(1-2):153-71.
88. Steimer JL, Mallet A, Golmard JL, Boisvieux JF. Alternative approaches to estimation of population pharmacokinetic parameters: comparison with the nonlinear mixed-effect model. Drug Metab Rev. 1984;15(1-2):265-92.
89. Karlsson MO, Beal SL, Sheiner LB. Three new residual error models for population PK/PD analyses. J Pharmacokinet Biopharm. 1995 Dec;23(6):651-72.
90. Waxman DJ, Azaroff L. Phenobarbital induction of cytochrome P-450 gene expression. Biochem J. 1992 Feb 1;281 (Pt 3):577-92.

91. Shimada M, Murayama N, Yamauchi K, Yamazoe Y, Kato R. Suppression in the expression of a male-specific cytochrome P450, P450-male: difference in the effect of chemical inducers on P450-male mRNA and protein in rat livers. Arch Biochem Biophys. 1989 May 1;270(2):578-87.
92. Riva R, Albani F, Contin M, Baruzzi A. Pharmacokinetic interactions between antiepileptic drugs. Clinical considerations. Clin Pharmacokinet. 1996 Dec;31(6):470-93.
93. Anderson GD. A mechanistic approach to antiepileptic drug interactions. Ann Pharmacother. 1998 May;32(5):554-63.
94. Paibir SG, Soine WH, Thomas DF, Fisher RA. Phenobarbital N-glucosylation by human liver microsomes. Eur J Drug Metab Pharmacokinet. 2004 Jan-Mar;29(1):51-9.
95. Kerr BM, Thummel KE, Wurden CJ, Klein SM, Kroetz DL, Gonzalez FJ, et al. Human liver carbamazepine metabolism. Role of CYP3A4 and CYP2C8 in 10,11-epoxide formation. Biochem Pharmacol. 1994 Jun 1;47(11):1969-79.
96. Parker AC, Pritchard P, Preston T, Choonara I. Induction of CYP1A2 activity by carbamazepine in children using the caffeine breath test. Br J Clin Pharmacol. 1998 Feb;45(2):176-8.
97. Waxman DJ. Interactions of hepatic cytochromes P-450 with steroid hormones. Regioselectivity and stereospecificity of steroid metabolism and hormonal regulation of rat P-450 enzyme expression. Biochem Pharmacol. 1988 Jan 1;37(1):71-84.
98. Imaoka S, Yamada T, Hiroi T, Hayashi K, Sakaki T, Yabusaki Y, et al. Multiple forms of human P450 expressed in Saccharomyces cerevisiae. Systematic characterization and comparison with those of the rat. Biochem Pharmacol. 1996 Apr 26;51(8):1041-50.
99. Sonderfan AJ, Arlotto MP, Dutton DR, McMillen SK, Parkinson A. Regulation of testosterone hydroxylation by rat liver microsomal cytochrome P-450. Arch Biochem Biophys. 1987 May 15;255(1):27-41.
100. Ryan DE, Levin W. Purification and characterization of hepatic microsomal cytochrome P-450. Pharmacol Ther. 1990;45(2):153-239.
101. Waxman DJ, Ko A, Walsh C. Regioselectivity and stereoselectivity of androgen hydroxylations catalyzed by cytochrome P-450 isozymes purified from phenobarbital-induced rat liver. J Biol Chem. 1983 Oct 10;258(19):11937-47.
102. Rodrigues AD, Prough RA. Induction of cytochromes P450IA1 and P450IA2 and measurement of catalytic activities. Methods Enzymol. 1991;206:423-31.
103. Thummel KE, Shen DD, Podoll TD, Kunze KL, Trager WF, Hartwell PS, et al. Use of midazolam as a human cytochrome P450 3A probe: I. In vitro-in vivo correlations in liver transplant patients. J Pharmacol Exp Ther. 1994 Oct;271(1):549-56.
104. Drescher S, Glaeser H, Murdter T, Hitzl M, Eichelbaum M, Fromm MF. P-glycoprotein-mediated intestinal and biliary digoxin transport in humans. Clin Pharmacol Ther. 2003 Mar;73(3):223-31.
105. Meijer J, Bergstrand A, DePierre JW. Preparation and characterization of subcellular fractions from the liver of C57B1/6 mice, with special emphasis on their suitability for use in studies of epoxide hydrolase activities. Biochem Pharmacol. 1987 Apr 1;36(7):1139-51.
106. Lowry OH, Rosebrough NJ, Farr AL, Randall RJ. Protein measurement with the Folin phenol reagent. J Biol Chem. 1951 Nov;193(1):265-75.
107. Tomson T, Tybring G, Bertilsson L, Ekbom K, Rane A. Carbamazepine therapy in trigeminal neuralgia: clinical effects in relation to plasma concentration. Arch Neurol. 1980 Nov;37(11):699-703.
108. Tachibana S, Tanaka M. Simultaneous determination of testosterone metabolites in liver microsomes using column-switching semi-microcolumn high-performance liquid chromatography. Anal Biochem. 2001 Aug 15;295(2):248-56.
109. Kushida K, Chiba K, Ishizaki T. Simultaneous liquid chromatographic determination of chloramphenicol and antiepileptic drugs (phenobarbital, phenytoin, carbamazepine, and primidone) in plasma. Ther Drug Monit. 1983;5(1):127-33.

110. Leclercq I, Desager JP, Vandenplas C, Horsmans Y. Fast determination of low-level cytochrome P-450 1A1 activity by high-performance liquid chromatography with fluorescence or visible absorbance detection. J Chromatogr B Biomed Appl. 1996 Jun 7;681(2):227-32.
111. Yao M, Zhang H, Chong S, Zhu M, Morrison RA. A rapid and sensitive LC/MS/MS assay for quantitative determination of digoxin in rat plasma. J Pharm Biomed Anal. 2003 Aug 21;32(6):1189-97.
112. Beal SL, Sheiner LS. NONMEM user's guides. Hanover, Maryland, GloboMax Inc.; 1989-1998.
113. Wahlby U, Jonsson EN, Karlsson MO. Assessment of actual significance levels for covariate effects in NONMEM. J Pharmacokinet Pharmacodyn. 2001 Jun;28(3):231-52.
114. Jonsson EN, Karlsson MO. Xpose--an S-PLUS based population pharmacokinetic/pharmacodynamic model building aid for NONMEM. Comput Methods Programs Biomed. 1999 Jan;58(1):51-64.
115. Lindbom L, Pihlgren P, Jonsson EN. PsN-Toolkit--a collection of computer intensive statistical methods for non-linear mixed effect modeling using NONMEM. Comput Methods Programs Biomed. 2005 Sep;79(3):241-57.
116. Boker KH, Franzen A, Wrobel M, Bahr MJ, Tietge U, Manns MP. Regulation of hepatic blood flow in patients with liver cirrhosis and after liver transplantation. Pathophysiology. 2000;6:251-60.
117. Jostell KG, Agurell S, Allgen LG, Kuylenstierna B, Lindgren JE, Aberg G, et al. Pharmacokinetics of clomethiazole in healthy adults. Acta Pharmacol Toxicol (Copenh). 1978 Sep;43(3):180-9.
118. Eichelbaum M, Kothe KW, Hoffman F, von Unruh GE. Kinetics and metabolism of carbamazepine during combined antiepileptic drug therapy. Clin Pharmacol Ther. 1979 Sep;26(3):366-71.
119. Thummel KE, O'Shea D, Paine MF, Shen DD, Kunze KL, Perkins JD, et al. Oral first-pass elimination of midazolam involves both gastrointestinal and hepatic CYP3A-mediated metabolism. Clin Pharmacol Ther. 1996 May;59(5):491-502.
120. Nakshabendi IM, McKee R, Downie S, Russell RI, Rennie MJ. Rates of small intestinal mucosal protein synthesis in human jejunum and ileum. Am J Physiol. 1999 Dec;277(6 Pt 1):E1028-31.
121. de Vries JX, Rudi J, Walter-Sack I, Conradi R. The determination of total and unbound midazolam in human plasma. A comparison of high performance liquid chromatography, gas chromatography and gas chromatography/mass spectrometry. Biomed Chromatogr. 1990 Jan;4(1):28-33.
122. Yamano K, Yamamoto K, Katashima M, Kotaki H, Takedomi S, Matsuo H, et al. Prediction of midazolam-CYP3A inhibitors interaction in the human liver from in vivo/in vitro absorption, distribution, and metabolism data. Drug Metab Dispos. 2001 Apr;29(4 Pt 1):443-52.
123. Lelo A, Birkett DJ, Robson RA, Miners JO. Comparative pharmacokinetics of caffeine and its primary demethylated metabolites paraxanthine, theobromine and theophylline in man. Br J Clin Pharmacol. 1986 Aug;22(2):177-82.
124. Lelo A, Miners JO, Robson RA, Birkett DJ. Quantitative assessment of caffeine partial clearances in man. Br J Clin Pharmacol. 1986 Aug;22(2):183-6.
125. Whalley PM, Bakes D, Grime K, Weaver RJ. Rapid high-performance liquid chromatographic method for the separation of hydroxylated testosterone metabolites. J Chromatogr B Biomed Sci Appl. 2001 Sep 5;760(2):281-8.
126. Bentley P, Oesch F. Foreign compound metabolism in the liver. Prog Liver Dis. 1982;7:157-78.

127. Owens IS. Genetic regulation of UDP-glucuronosyltransferase induction by polycyclic aromatic compounds in mice. Co-segregation with aryl hydrocarbon (benzo(alpha)pyrene) hydroxylase induction. J Biol Chem. 1977 May 10;252(9):2827-33.
128. Hagbjörk A-L, Ågren J, Andersson A, Terelius Y. In Vitro Metabolism of Clomethiazole by Human Liver Microsomes and Human Cytochrome P450 Isoforms. Drug Metab Rev. 2003;35, Suppl 1:1-168.
129. Fuhr U, Rost KL, Engelhardt R, Sachs M, Liermann D, Belloc C, et al. Evaluation of caffeine as a test drug for CYP1A2, NAT2 and CYP2E1 phenotyping in man by in vivo versus in vitro correlations. Pharmacogenetics. 1996 Apr;6(2):159-76.
130. Centerholt C, Ekblom M, Odergren T, Borga O, Popescu G, Molz KH, et al. Pharmacokinetics and sedative effects in healthy subjects and subjects with impaired liver function after continuous infusion of clomethiazole. Eur J Clin Pharmacol. 2003 Jun;59(2):117-22.
131. Oscarson M, Zanger UM, Rifki OF, Klein K, Eichelbaum M, Meyer UA. Transcriptional profiling of genes induced in the livers of patients treated with carbamazepine. Clin Pharmacol Ther. 2006 Nov;80(5):440-56 e7.
132. Ghanbari F, Rowland-Yeo K, Bloomer JC, Clarke SE, Lennard MS, Tucker GT, et al. A critical evaluation of the experimental design of studies of mechanism based enzyme inhibition, with implications for in vitro-in vivo extrapolation. Curr Drug Metab. 2006 Apr;7(3):315-34.
133. Kalow W, Tang BK. The use of caffeine for enzyme assays: a critical appraisal. Clin Pharmacol Ther. 1993 May;53(5):503-14.

Acta Universitatis Upsaliensis

Digital Comprehensive Summaries of Uppsala Dissertations from the Faculty of Pharmacy 52

Editor: The Dean of the Faculty of Pharmacy

A doctoral dissertation from the Faculty of Pharmacy, Uppsala University, is usually a summary of a number of papers. A few copies of the complete dissertation are kept at major Swedish research libraries, while the summary alone is distributed internationally through the series Digital Comprehensive Summaries of Uppsala Dissertations from the Faculty of Pharmacy. (Prior to January, 2005, the series was published under the title "Comprehensive Summaries of Uppsala Dissertations from the Faculty of Pharmacy".)

Distribution: publications.uu.se
urn:nbn:se:uu:diva-7812

ACTA
UNIVERSITATIS
UPSALIENSIS
UPPSALA
2007